Gondwana Large Igneous Provinces: plate reconstructions, volcanic basins and sill volumes

H. H. SVENSEN[1]*, T. H. TORSVIK[1,2,3,4], S. CALLEGARO[1], L. AUGLAND[1], T. H. HEIMDAL[1], D. A. JERRAM[1,5], S. PLANKE[1,6] & E. PEREIRA[7]

[1]*Centre for Earth Evolution and Dynamics (CEED), University of Oslo, PO Box 1028, Blindern, 0316 Oslo, Norway*

[2]*Geodynamics, Geologiske Undersøkelse (NGU), Leiv Eirikssons Vei 39, N-7491 Trondheim, Norway*

[3]*School of Geosciences, University of Witwatersrand, Johannesburg, WITS 2050, South Africa*

[4]*GFZ German Research Centre for Geosciences, Telegrafenberg, 14473 Potsdam, Germany*

[5]*DougalEARTH Ltd, 31 Whitefields Crescent, Solihull B91 3NU, UK*

[6]*Volcanic Basin Petroleum Research (VBPR), Oslo Science Park, Gaustadalléen 21, N-0349 Oslo, Norway*

[7]*Department of Stratigraphy and Paleontology, Rio de Janeiro State University, Brazil*

**Correspondence: hensven@geo.uio.no*

Abstract: Gondwana was an enormous supertarrane. At its peak, it represented a landmass of about 100×10^6 km^2 in size, corresponding to approximately 64% of all land areas today. Gondwana assembled in the Middle Cambrian, merged with Laurussia to form Pangea in the Carboniferous, and finally disintegrated with the separation of East and West Gondwana at about 170 Ma, and the separation of Africa and South America around 130 Ma. Here we have updated plate reconstructions from Gondwana history, with a special emphasis on the interactions between the continental crust of Gondwana and the mantle plumes resulting in Large Igneous Provinces (LIPs) at its surface. Moreover, we present an overview of the subvolcanic parts of the Gondwana LIPs (Kalkarindji, Central Atlantic Magmatic Province, Karoo and the Paraná–Etendeka) aimed at summarizing our current understanding of timings, scale and impact of these provinces. The Central Atlantic Magmatic Province (CAMP) reveals a conservative volume estimate of 700 000 km^3 of subvolcanic intrusions, emplaced in the Brazilian sedimentary basins (58–66% of the total CAMP sill volume). The detailed evolution and melt-flux estimates for the CAMP and Gondwana-related LIPs are, however, poorly constrained, as they are not yet sufficiently explored with high-precision U–Pb geochronology.

The Gondwana supertarrane had a surface area of about 100×10^6 km^2, and was assembled in Late Neoproterozoic and Cambrian times. It later amalgamated with Laurussia to form Pangea in the Late Carboniferous. Gondwana (or Gondwanaland) was first named by Medlicott & Blanford (1879), and included most of South America, Africa, Madagascar, India, Arabia, East Antarctica and Western Australia (Torsvik & Cocks 2013). Gondwana was affected by several Large Igneous Provinces (LIPs) from the Cambrian to its final break-up in the Cretaceous. These LIPs were likely to have been sourced from mantle plumes, and had major impacts on deep and shallow crustal rheology and on the Earth's climate. In general, the structure of the LIPs is two-fold, with (1) surface lava flows and pyroclastic deposits, and (2) a network of subvolcanic sills and dykes. The latter were commonly emplaced in sedimentary basins, and thus led to a wide range of effects including metamorphism, devolatilization, porosity reduction, and phreatic and phreatomagmatic eruptions.

The aim of this paper is to present plate reconstructions of the evolution of Gondwana, and to assess the timing and consequences of LIP formation. This is of great interest since Gondwana continental LIPs are associated with both major mass extinctions and rapid climatic changes. We stress that our contribution is not meant as a comprehensive review but as an update on key periods of the

From: Sensarma, S. & Storey, B. C. (eds) *Large Igneous Provinces from Gondwana and Adjacent Regions*. Geological Society, London, Special Publications, **463**, https://doi.org/10.1144/SP463.7

long Gondwana history (pertaining to the LIPs: Kalkarindji, Central Atlantic Magmatic Province, Karoo and the Paraná–Etendeka), and a useful summary of our current understanding. We put a special emphasis on the emplacement environments of the subvolcanic parts of the LIPs, in particular of the Central Atlantic Magmatic Province (CAMP) and the affected sedimentary basins, as this theme is poorly known outside the Brazilian geological community.

Methods

Plate reconstructions

We used GPlates (www.gplates.org; and GMAP (Torsvik & Smethurst 1999) for plate reconstructions and data analysis. Mesozoic reconstructions use a palaeomagnetic reference frame based on the zero Africa longitude method (Torsvik *et al.* 2012), whilst our Cambrian reconstruction is detailed in Torsvik *et al.* (2014). The lower mantle is dominated by two equatorial and antipodal regions of low seismic shear-wave velocities, referred to as the Large Low Shear-wave Velocity Provinces (LLSVPs), or using more friendly acronyms of Kevin Burke, TUZO (the LLSVP beneath Africa) and JASON (its Pacific counterpart). TUZO and JASON are prominent in all global shear-wave tomographic models, and most reconstructed Large Igneous Provinces (LIPs) and kimberlites over the past 300 myr – and perhaps much longer (Torsvik *et al.* 2014, 2016) – have erupted directly above their margins, termed the plume generation zones (PGZs: Burke *et al.* 2008). In order to relate deep-mantle processes to surface processes in a palaeomagnetic reference frame, we have counter-rotated the PGZs to account for true polar wander (TPW). Here we use the 0.9% slow contour in the tomographic shear-wave model (s10mean: Doubrovine *et al.* 2016) as the best approximation of the plume source region in the deep mantle. This is shown in Figures 1–3, where the location of the PGZ (thick red line) is corrected for TPW. In this way, we apply estimated TPW rotations (Torsvik *et al.* 2014) to the mantle to simultaneously visualize how the reconstructed continents and the underlying mantle structures would look like in the palaeogeographical reference frame (Torsvik & Cocks 2013)

Geochronology

Most of the LIPs described here (see Table 1) have been dated by high-precision zircon U–Pb chemical abrasion isotope dilution thermal ionization mass spectrometry (CA-ID-TIMS) geochronology, with the use of a common U–Pb tracer allowing direct interlaboratory data comparison (i.e. the EARTHTIME tracer: Condon *et al.* 2015). The CA-ID-TIMS data from the Paraná part of the Paraná–Etendeka LIP (Janasi *et al.* 2011; Florisbal *et al.* 2014) and the data from Svensen *et al.* (2012) from the Karoo used in-house U–Pb tracers, but the tracer used in the latter study has been calibrated to the EARTHTIME tracer (Svensen *et al.* 2015*a*; Corfu *et al.* 2016). There are no U–Pb data from the Etendeka part of the Paraná–Etendeka LIP, so only $^{40}Ar/^{39}Ar$ ages are reported (corrected to the latest standards). We have not included ion microprobe (SIMS/SHRIMP) and laser ablation inductively coupled plasma mass spectrometry (LA-ICP-MS) data as these methods do not yield ages with the required precision to evaluate potential correlations of short-lived geological events (e.g. LIP magmatism and mass extinction events). Furthermore, due to the relatively low level of precision of the data, potential Pb-loss is difficult to constrain, again leading to large uncertainties regarding the accuracy of ages. Similarly, baddeleyite ages are generally left out of this review – unless they are combined with zircon and, hence, can be evaluated relative to zircon data – as these are also prone to Pb loss if not abraded (for a discussion of potential problems with baddeleyite ages, see, e.g., Corfu *et al.* 2016). All the zircon U–Pb ID-TIMS ages considered are reported, including tracer calibration uncertainties and excluding decay constants uncertainties, and are shown in Figure 4. For comparison, $^{40}Ar/^{39}Ar$ age ranges (recalculated to conform to the Fish Canyon sanidine age of Kuiper *et al.* 2008) are also included in Figure 4, as these ages represent the majority of analyses for several of the LIPs and has, in some cases, been used to argue for longevity of magmatic activity (e.g. Jourdan *et al.* 2005).

Basin-scale sill volume estimates

Total sill volumes from the sedimentary basins are notoriously difficult to estimate. Our approach is similar to that of Svensen *et al.* (2015*b*) from the Karoo Basin, using the aerial extent of the relevant basins and borehole-based sill thicknesses. Data from the literature (chiefly, outcrop, borehole and seismic data) were then scouted and used to estimate the total cumulative thickness of sills in the basins. Thicknesses of the sills are likely to vary across the basins, commonly with maxima at the centres; thus, minimum, maximum and mean thicknesses were used to calculate the total volume. We argue that the mean thickness is the most reasonable value to be used for estimating sill volumes in sedimentary basins, but minimum and maximum volumes are also reported in order to show the total range of plausible values. We summarize the literature-based sill volume estimates in Table 2, and our new CAMP compilation in Table 3, followed by a separate CAMP section in the Results.

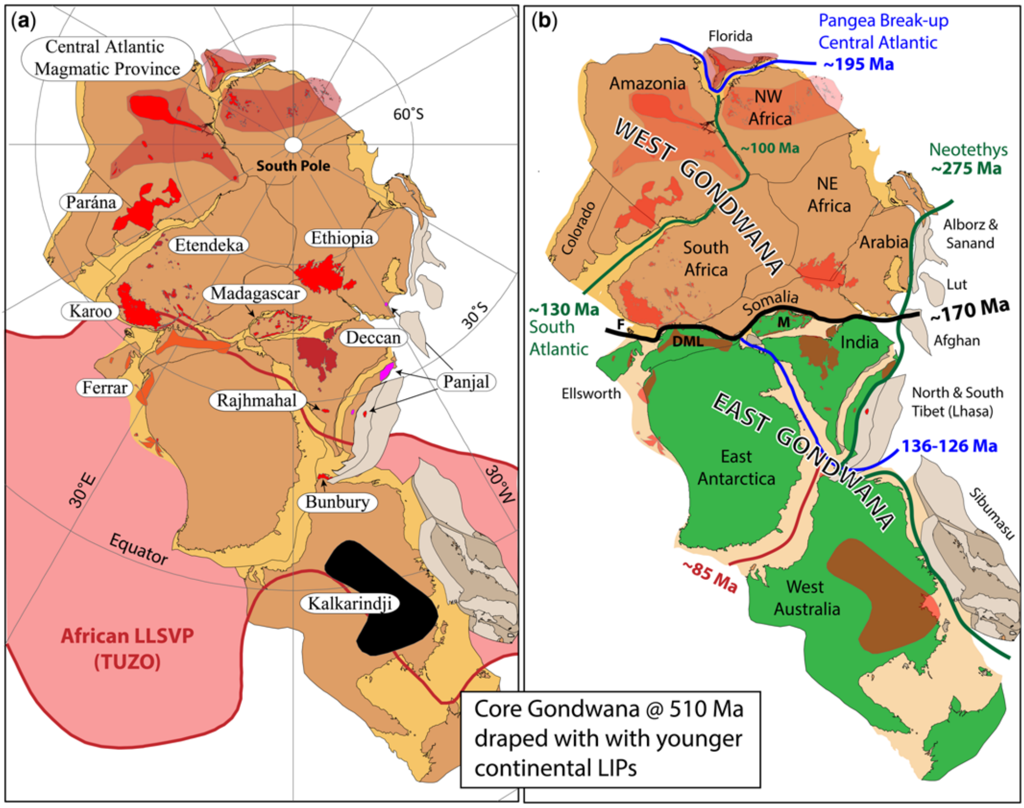

Fig. 1. (**a**) Reconstruction of core Gondwana at 510 Ma (Torsvik *et al.* 2014), around the time when the Kalkarindji LIP (black outline) erupted in Western Australia above the margin of TUZO (African Large Low Shear-wave Velocity Province; LLSVP). Also shown are all younger continental LIPs that affected Gondwana continental crust (see Table 1). (**b**) Similar to (a) but highlighting some important phases of Gondwana dispersal until the Early Cretaceous. The main break-up of Gondwana started at some time after 170 Ma when West and East Gondwana (green shading) separated. Peri-Gondwanan terranes that drifted off Gondwana (as part of Pangea) in the Early Permian (opening of Neotethys) are shaded in grey. F, Falkland; DML, Dronning Maud Land; M, Madagascar.

Results

The birth and demise of Gondwana

Unification of the many old cratons and terranes to form Gondwana began in the Late Neoproterozoic and continued into the Cambrian, but was largely over before the Middle Cambrian. The core of Gondwana included most of South America, Africa, Madagascar, India, Arabia, East Antarctica and Western Australia (Torsvik & Cocks 2013), and it reached a size of about 100×10^6 km^2 at its maximum (*c.* 64% of all land areas today). There were also many smaller units along its margins, such as Avalonia (including England), which had already drifted away during the Early Ordovician (with opening of the Rheic Ocean).

Gondwana merged with Laurussia (Laurentia, Baltica and Avalonia) in the Carboniferous at around 320 Ma to form Pangea. The disintegration of Gondwana had already started in the Early Ordovician but its demise after the Pangea assembly (Fig. 1) can be summarized as follows:

- Opening of the Neotethys from about 275 to 260 Ma, when a string of microcontinents and terranes such as Alborz and Sanand (Iran) through to Lut, Afghanistan, Tibet and Sibumasu moved away from the eastern rim of the Gondwanan sector of Pangea.
- Opening of the Central Atlantic at around 195 Ma. This led to the definite break between North and South Pangea, with the result that the core Gondwanan continent regained its independence for 20–30 myr. Florida was left behind with North America.
- Separation of East and West Gondwana at around 170 Ma; this is essentially the demise

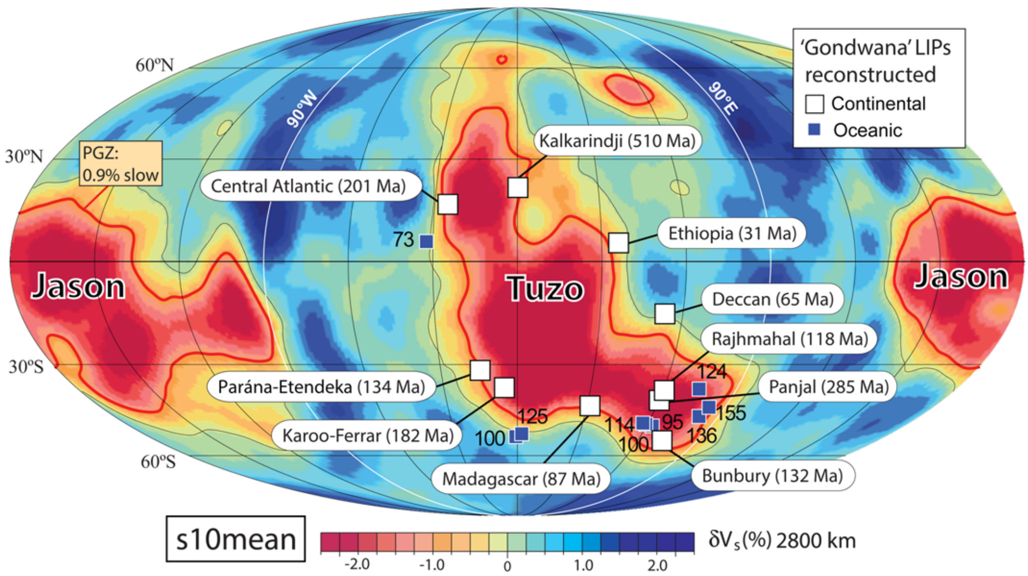

Fig. 2. Reconstruction of all 'Gondwana'-related Phanerozoic LIPs (31–510 Ma) using a hybrid reference frame (Torsvik *et al.* 2016) and draped on the s10mean tomographic model of Doubrovine *et al.* (2016). The plume generation zone (PGZ) in this model corresponds to the 0.9% slow contour. LIPs with white-squared symbols are continental LIPs, whilst those with blue-squared symbols are oceanic plateaus (LIP numbers are ages in Ma: see Table 1).

of Gondwana, but other important break-up phases that involved Gondwana continental crust included the East Gondwana break-up, starting with a separation between East Antarctica–Australia from India between 136 and 126 Ma, and the West Gondwana break-up, starting with opening of the South Atlantic at around 134 Ma.

Other younger but important post-Gondwana break-up phases include: (i) departure of India/Seychelles from Madagascar (opening of the Mascarene Basin) at around 84 Ma; (ii) East Antarctica and Australia separating at *c.* 85 Ma; (iii) India and Seychelles separating at 62–63 Ma; and (iv) departure of Arabia from Africa (opening of the Red Sea). This probably started with an early short-lived phase of seafloor spreading at around 26 Ma, and saw the onset of a second and still ongoing phase of seafloor spreading in the Pliocene, about 5 myr ago.

Constraining volumes: CAMP volcanism and sills in Brazil

Despite the growing amount of literature pertaining to the CAMP event, a thorough assessment of the preserved and original volumes of CAMP products is still lacking, with the only exception being a contribution by McHone (2003). In general, a total pre-erosional volume of 2.5×10^6 km^3 is addressed (e.g. Marzoli *et al.* 1999*b*). The total volume of magmatic products emplaced by the CAMP is within the same order of magnitude of those of other Large Igneous Provinces, but the general thickness (of outpoured material) is estimated as being smaller (Sebai *et al.* 1991; McHone 2003). Before we discuss the role of LIPs in the evolution and break-up of Gondwana, we would like to address the lack of constraint on the volumes associated with the CAMP event.

In general, intrusive and subvolcanic magmatism seems to constitute a large portion of the CAMP event. The only published estimates for volumes of CAMP products and relative degassing (McHone 2003) do not consider the existence of: (i) CAMP intrusions; (ii) Bolivian, Moroccan and Iberian CAMP occurrences (Knight *et al.* 2004; Bertrand *et al.* 2014; Callegaro *et al.* 2014); and (iii) an underestimate the extent of vast sills from Taoudenni–Hank–Reggane basins in Mali and Algeria (Verati *et al.* 2005; Charaf Chabou *et al.* 2010), from the Fouta Djalon Plateau (Deckart *et al.* 2005), and South America. Here we estimate the original volume of the CAMP starting from what is the present-day volume and surface of CAMP relicts. Particular emphasis is put on the sills and the intrusions, partly because the only available estimates to date are mainly focused on the lava piles, and partly because intrusive and subvolcanic bodies yield a high potential for degassing volatiles able to impact the global

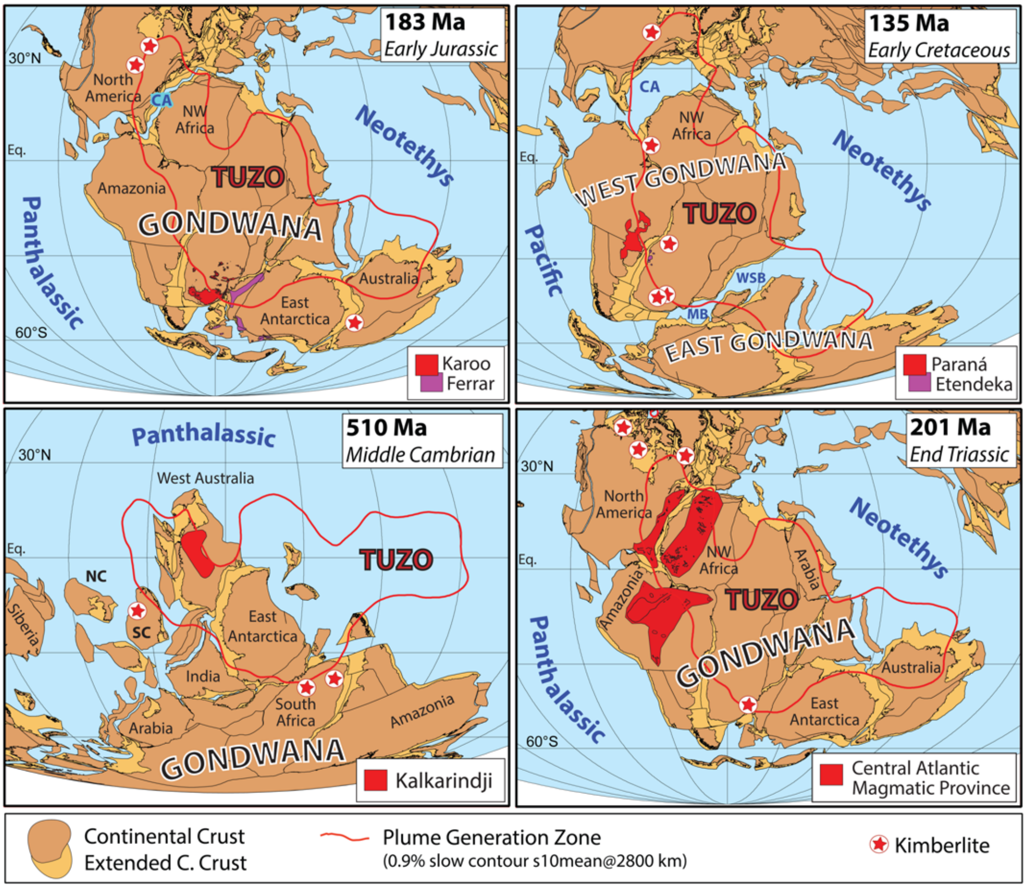

Fig. 3. Reconstructions at 510 Ma (Kalkarindji), 201 Ma (Central Atlantic Magmatic Province), 183 Ma (Karoo and Ferrar) and 135 Ma (134?: Paraná–Etendeka). These are palaeomagnetic reconstructions (Torsvik *et al.* 2012, 2014) but the plume generation zones has been counter-rotated to account for true polar wander. We have also reconstructed kimberlites within ±5 Ma for each reconstruction interval. CA, Central Atlantic; MB, Mozambique Basin; NC, North China; SC, South China; WSB, West Somali Basin.

environment (e.g. Svensen *et al.* 2004, 2009; Ganino & Arndt 2009; Aarnes *et al.* 2010), making them significant in the broader picture of understanding the relationship between CAMP and the end-Triassic mass extinction (Marzoli *et al.* 2004; Blackburn *et al.* 2013).

Products of extensive subvolcanic CAMP magmatism are present in northern Brazil, as thick doleritic sheets emplaced within the Palaeozoic sediments of the extensive Amazonas (*c.* 5×10^5 km^2), Solimões (*c.* $4 \times 10^5 - 6 \times 10^5$ km^2) and Acre basins (2.3×10^5 km^2: Milani & Zalán 1999; De Min *et al.* 2003) (Fig. 5). The stratigraphy of these deep (down to 5 km) intracontinental sedimentary basins includes three or four Palaeozoic supersequences of mainly siliciclastic rocks, along with thick (up to 1600 m: Milani & Zalán 1999) Carboniferous–Permian evaporitic and carbonate deposits. CAMP sills intruded Carboniferous–Permian evaporites and carbonates in the Solimões Basin, whereas, in the Amazonas Basin, sills are recorded both in Ordovician–Carboniferous siliciclastic sediments and in Carboniferous–Permian evaporites (Wanderley Filho *et al.* 2006). The maximum cumulative sill thickness (1038 m: Wanderley Filho *et al.* 2006) is reached in the Solimões Basin, and this decreases both eastwards towards the Amazonas Basin (between 100 and 809 m) (Fig. 5) and westwards towards the Acre Basin (Almeida 1986; De Min *et al.* 2003). The sill emplacement depth for the Brazilian basins typically varies between 1000 and 3500 m (Wanderley Filho *et al.* 2006) (Fig. 5). Affiliation to the CAMP of intrusive rocks found within the 600 000 km^2-wide Parnaíba sedimentary basin is questionable given the substantial spread in K–Ar ages shown by these rocks (Mizusaki *et al.*

Table 1. *Phanerozoic Large Igneous Provinces (LIPs) linked to 'Gondwana' and its dispersal history*

Continental	Age (Ma)	Oceanic plateaus	Age (Ma)
Ethiopia	31	Sierra Leone Rise	73
Deccan Traps	65	Broken Ridge	95
Madagascar	87	Central Kerguelen	100
Rajhmahal Traps	118	Agulhas Plateau	100
Bunbury Basalts–Cuvier–Gascoyne	132	Southern Kerguelen	114
Paraná–Etendeka	134	Wallaby Plateau	124
Argo Margin	155	Maud Rise	125
Karoo	182		
Central Atlantic Magmatic Province	201		
Panjal Traps	285		
Kalkarindji	510		

LIPs are separated into continental (see Fig. 1) and oceanic plateaus (Fig. 2).

2002). On the other hand, the presence of lava flows of clear CAMP age (Mosquito Formation: De Min *et al.* 2003; Merle *et al.* 2011) overlying the Palaeozoic sedimentary sequences in the Parnaíba Basin (the only known extrusive components of CAMP magmatism in Brazil: Marzoli *et al.* 1999*b*) may indicate that at least some of the dolerite sheets (Porto & Pereira 2014) recorded in the boreholes are CAMP related. The Parnaíba Basin does, however, host sills of undoubted Paraná–Etendeka affinity (Mizusaki *et al.* 2002; Porto & Pereira 2014) within its up to 3500 m-thick Palaeozoic sediments (siliciclastic and calcareous-evaporitic: Milani & Zalán 1999).

CAMP sills are often cropping out in restricted areas in sedimentary basins (outcrops cover *c.* 20% of the total), but borehole data from the basins generally intercept dolerites resting underneath most of the basin surface (cf., e.g., the Taoudenni Basin or the Brazilian basins: Milani & Zalán 1999; Verati *et al.* 2005). Boreholes and seismic data often reveal several sills stacked at different levels of the sedimentary pile (Fig. 5). We thus calculated the volume of CAMP sills by considering the extension of the basins that host them multiplied by the cumulative thickness of the doleritic sheets (Fig. 6; Table 3). Depending on the structure of the basin, the thickness of the sills can vary from the centre to the edges, tapering towards both ends of the basin (e.g. within the Amazon Basin: Fig. 5) or as a regional trend (e.g. thickness waning east and west of the Solimões Basin: De Min *et al.* 2003), resulting in high uncertainty for the thickness estimation. Therefore, we calculated the minimum, average and maximum volumes by considering the variability related to the sill thickness (Table 3). The total estimated volume of CAMP products approaches 1×10^6 km^3 if the average thickness of sills and in-basin flows is considered. If a less conservative estimate is used, the total subvolcanic volume exceeds 1.6×10^6 km^3.

It should be noted that these calculated volumes hinge on the extension of sedimentary basins and observation of the magmatic products preserved within them. Therefore, the better preservation of sills with respect to lava flows may lead to a disparity between intrusive and extrusive volumes that might not reflect the original proportion of CAMP products. While sills volume are well constrained through this method, lava-flow volumes should be taken as minimum estimates, since CAMP lava fields might have extended above all those regions presently cut by the dyke swarms (cf. McHone 2003). We decided to limit the calculations to basin areas because of the better-constrained information we have for these settings in the present: that is, being target to sedimentation, they are proven to be depocentres, capable of accommodating significant volumes of lava flows. Also, further potential CAMP occurrences are known to exist in remote areas of Africa and South America, but we here limit out assessment to the CAMP occurrences for which some (geochronological and/or geochemical) data have been published: that is, for which a CAMP affiliation was demonstrated. Therefore, we stress that these estimates are rather conservative and that future studies on the CAMP might result in larger volume estimates for this LIP.

Discussion

The major LIPs of Gondwana

Gondwana is not only unique for having been the largest unit of continental crust on Earth for more than 200 myr before its amalgamation with Laurussia in the Carboniferous to form Pangea, but also for hosting abundant LIPs. Around 30 Phanerozoic LIPs are commonly listed in global compilations, and 19 of these (11 continental and seven oceanic LIPs, Table 1) – 60% of all LIPs – affected Gondwanan continental lithosphere and its margins and oceanic lithosphere during Gondwana dispersal. Four case studies are discussed in this contribution, including the Cambrian Kalkarindji LIP in Western Australia, the end-Triassic CAMP that affected vast areas in North America, NW Africa and South America, the Early Jurassic Karoo–Ferrar LIP in South Africa and Antarctica (heralding the Jurassic

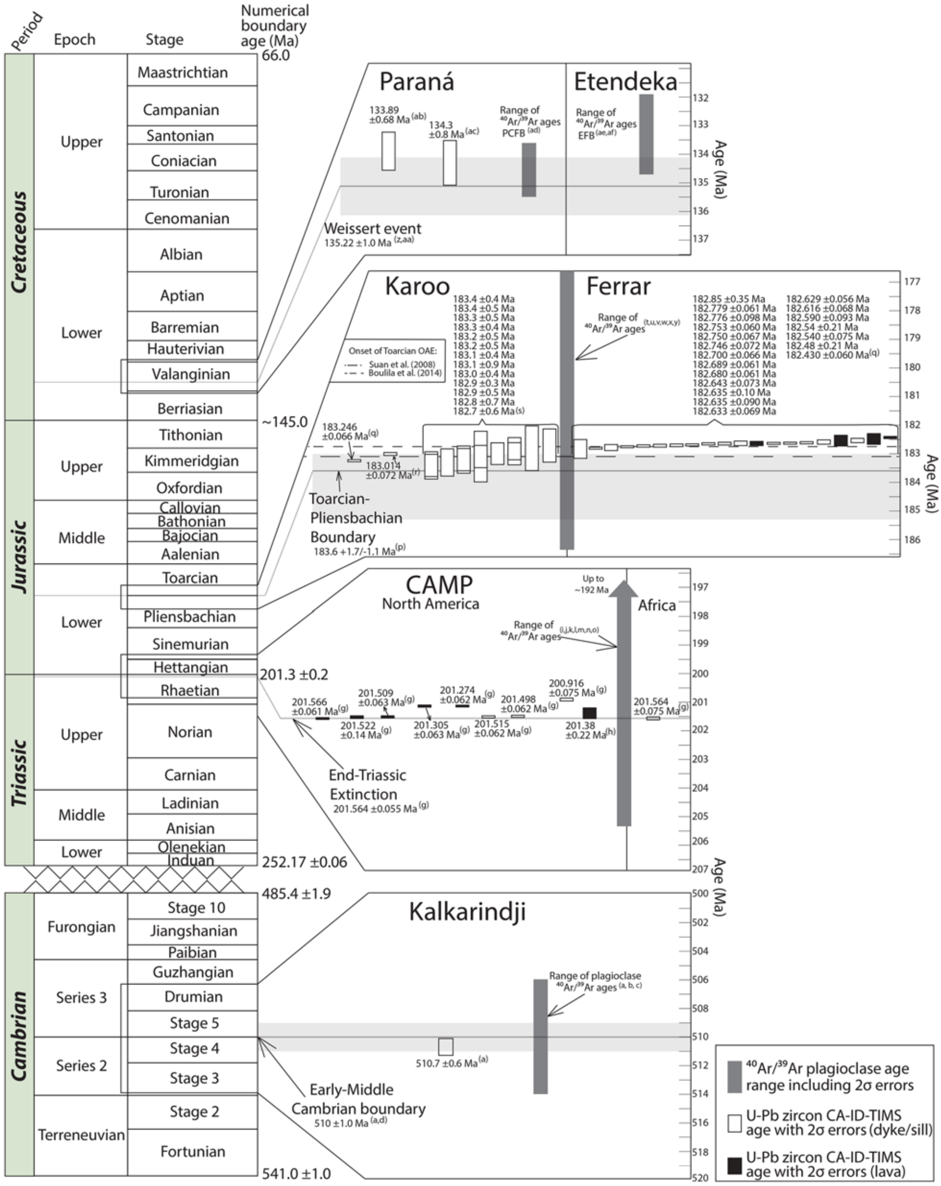

Fig. 4. Zircon U–Pb ID-TIMS and $^{40}Ar/^{39}Ar$ mineral data from the Central Atlantic Magmatic Province, the Karoo and Ferrar, and the Paraná–Etendeka Large Igneous Provinces. Uncertainties of all U–Pb ages reported include both the analytical uncertainty and the uncertainty derived from the tracer calibration, except for the data from Janasi *et al.* (2011) and Florisbal *et al.* (2014) where information on whether the tracer calibration uncertainties were included in the age calculations could not be obtained. The decay constant uncertainties are not included. Uncertainties on the reference events or boundaries in each panel are 2σ. The chronostratigraphic base chart is taken from Cohen *et al.* (2013; updated). The referred ages are taken from: (a) Jourdan *et al.* (2014); (b) Glass & Phillips (2006); (c) Evins *et al.* (2009); (d) Harvey *et al.* (2011); (e) Landing *et al.* (1998); (g) Blackburn *et al.* (2013); (h) Schoene *et al.* (2010); (i) Jourdan *et al.* (2009); (j) Nomade *et al.* (2007); (k) Hames *et al.* (2000); (l) Beutel *et al.* (2005); (m) Marzoli *et al.* (2011); (n) Knight *et al.* (2004); (o) Nomade *et al.* (2000); (q) Burgess *et al.* (2015); (r) Sell *et al.* (2014); (s) Svensen *et al.* (2012); (t) Jourdan *et al.* (2008); (u) Le Gall *et al.* (2002); (v) Jourdan *et al.* (2004); (w) Jourdan *et al.* (2005); (x) Jourdan *et al.* (2007*a*); (y) Jourdan *et al.* (2007b); (z) Martinez *et al.* (2015); (aa) Aguirre-Urreta *et al.* (2015); (ab) Florisbal *et al.* (2014); (ac) Janasi *et al.* (2011); (ad) Thiede & Vasconcelos (2010); (ae) Marzoli *et al.* (1999*a*); and (af) Renne *et al.* (1996). CAMP, Central Atlantic Magmatic Province; OAE, Oceanic Anoxic Event.

Table 2. *Major volcanic basins, Large Igneous Provinces (LIP), and environmental changes*

LIP	Comment	Correlated event	CIE*	Environmental changes	Biosphere changes	Sedimentary metamorphism	Sill age (Ma)	Sill volume (km^3)	References
Paraná–Etendeka	Paraná and Etendeka basins	Valanginian OAE	Positive	Cooling	limited	Sanstone/Shale	134		
	Paraná basin sills							112 000	4
	Etendeka sills and complexes							>10 000	This work
Karoo–Ferrar	Karoo Basin sills	Toarcian	Negative	Warming	Minor Extinction	Shale	182.6	370 000	1
	Antarctica sills					Sandstone + coal	182.6	170 000–230 000	2,3
	Tasmania sills							15 000	3
	All sills in the major basins							555 000–615 000	
CAMP	All affected basins	End-Triassic	Negative	Warming	Mass extinction	Evaporite + shale	201	700 000	This work
Siberian Traps	Tunguska Basin sills	End-Permian	Negative	Warming	Mass extinction	Evaporite + shale	252	780 000	5
Kalkarinji	Australia	Early–Middle Cambrian	Positive	OAE†	Mass extinction	Shale	510.7	?	

*CIE, Carbon Isotope Excursion.
†OAE, Oceanic Anoxic Event.
References: 1, Svensen *et al.* (2012); 2, Elliot & Fleming (2000); 3, Storey *et al.* (2013); 4, Frank *et al.* (2009); 5, Vasiliev *et al.* (2000).

Table 3. *Sedimentary basins with CAMP sills and their estimated volumes*

CAMP sills		Thickness (km)	Basin area (km^2)	Average volume (km^3)	Minimum volume (km^3)	Maximum volume (km^3)	References
North America	Newark Basin – Palisades (PA, NJ, NY)*	Up to 0.35	2400	480	240	840	1, 2, 3
	Culpeper Basin – Belmont, Rapidan sills (VA, MD)	0.37–0.6	2750	1380	550	1650	2, 4
	Gettysburg Basin York Haven sill (PA, MD)*	0.676	170	77	34	115	2, 4
	Deep River Basin – Sandford, Durham (NC, SC)	0.2	4000	800	200	1200	2, 3
	Dan River – Danville Basin (NC)	0.2	1500	300	75	450	2, 3
Africa	Anti Atlas (Morocco)	0.05–0.1	60 000	9000	6000	12 000	5
	Taoudenni (Mali)	0.2–0.4	100 000	30 000	20 000	40 000	5, 6
	Reggane, Tindouff, Hank (Mauritania, Algeria)	0.2–0.5	240 000	72 000	48 000	120 000	5
	Fouta Djalon (Guinea)	0.01–0.9	150 000	60 000	1500	135 000	7
South America	Acre (Brazil)	0.1–0.8	230 000	69 000	23 000	184 000	8
	Solimoes (Brazil)	Up to 1.038	400 000	200 000	40 000	400 000	8, 9
	Amazon (Brazil)	Up to 0.915	500 000	250 000	50 000	458 000	8, 9
	Tarabuco, Camiri (Bolivia)	0.03–0.14	30 000	2100	300	4200	10
	Devil’s Island (French Guyana)	0.035	13	0	–	–	9
Europe	Pyrenees ‘ophites’ (Spain, France)	0.05–0.2	35 000	3500	1750	17 500	11, 12
			1 760 000	699 000	192 000	1 370 000	

*For the Gettysburg and Newark basins, the reported area is not that of the entire basins but only the area of extension of the sills.
Data from: 1, Puffer *et al.* (2009); 2, McHone (2003); 3, Luttrell (1989); 4, Woodruff *et al.* (1995); 5, Charaf Chabou *et al.* (2010); 6, Verati *et al.* (2005); 7, Deckart *et al.* (2005); 8, De Min *et al.* (2003); 9, Milani & Zalán (1999); 10, Bertrand *et al.* (2014); 11, Béziat *et al.* (1991); 12, Callegaro *et al.* (2014).

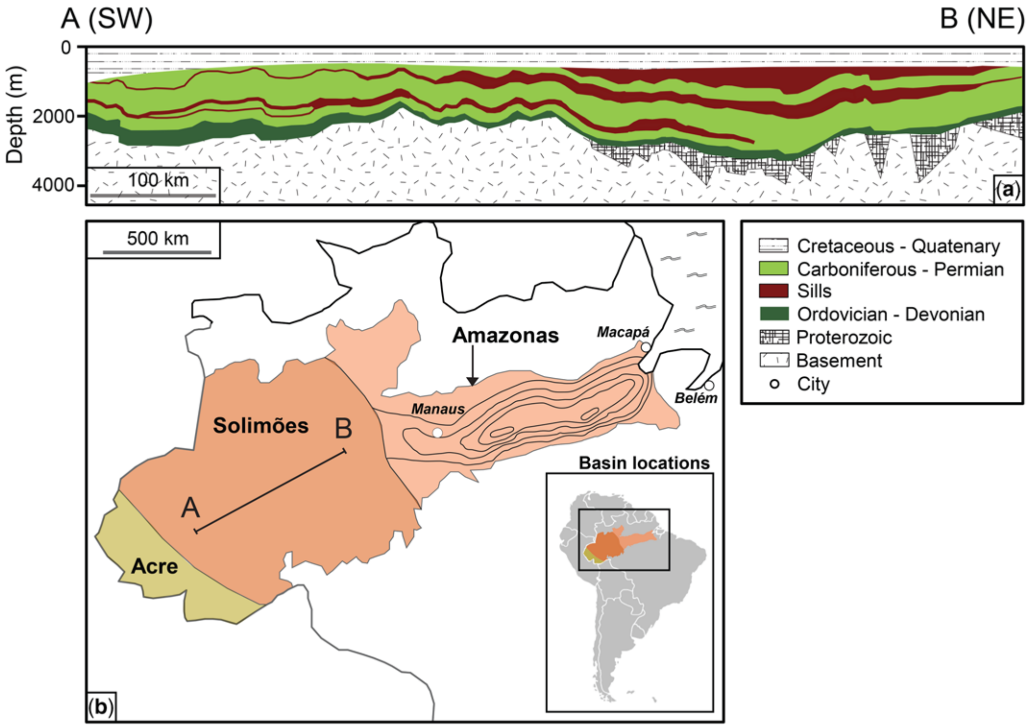

Fig. 5. (**a**) Qualitative SW–NE cross-section of the Solimões Basin (Brazil: A–B line marked in b highlights the presence of multiple thick sills encompassing the entire basin. (**b**) Outline of three Brazilian basins, Acre, Solimões and Amazon from west to east. Isopachs of cumulative sill thickness are marked for the Amazon Basin only (one line each 200 m in thickness, from 100 to 900 m). Adapted from Wanderley Filho *et al*. (2006).

break-up of Gondwana), and, finally, the Paraná–Etendeka LIP, which affected large areas in South America and SW Africa (e.g. Brazil, Namibia and Angola), and assisted the opening of the South Atlantic from around 134 Ma.

The Kalkarindji Large Igneous Province

In the early Palaeozoic, Gondwana stretched from the South Pole to the equator (West Australia) and the Kalkarindji continental flood basalt province erupted at equatorial latitudes (Figs 1 & 3). Kalkarindji is a relatively poorly known LIP located in the interior of Western Australia. The name of the province was originally proposed by Glass & Phillips (2006) to encompass the Early Cambrian basalts of the Antrim Plateau in northern Australia, and a number of smaller basalt and dolerite outcrops in the interior of the continent. Recent overviews of the province can be found in Ernst (2014) and www.largeigneousprovinces.org/LOM

The current extent of the Kalkarindji outcrops is about 55 000 km^2, with an estimated initial areal extent of 400 000 km^2 and a volume of 0.15×10^6 km^3 (Marshall *et al.* 2016 and references therein). The areal extent of the entire Kalkarindji province is estimated to be at least 2.1×10^6 km^2, but could be greater than 3×10^6 km^2 if igneous complexes in the Adelaide Fold Belt in South Australia are included as part of the province (Evins *et al.* 2009; Ernst 2014). The offshore extent of the province is currently unknown, but the Milliwindi dyke extends at least 70 km to the north of the Kimberly (Hanley & Wingate 2000). The volume of the erupted and associated shallow intrusive rocks is difficult to determine due to the scattered outcrops (see Fig. 7a), but is likely to be greater than 1.5×10^6 km^3 (Ernst 2014).

The igneous complexes of the Kalkarindji LIP consist dominantly of inflated, subaerial basalt flows and dolerite sheet intrusions. The basalts are dominantly low-Ti tholeiites and highly enriched in incompatible elements, suggesting continental contamination of the magmas (Glass & Phillips 2006; Ernst 2014). The most extensive and best-preserved basalt outcrops are located in the remote western part of the Antrim Plateau, reaching a thickness of at least 1.1 km. The lava flows are typically 20–60 m thick with massive interior and fractured or brecciated flow tops. Intraflow sedimentary units, including

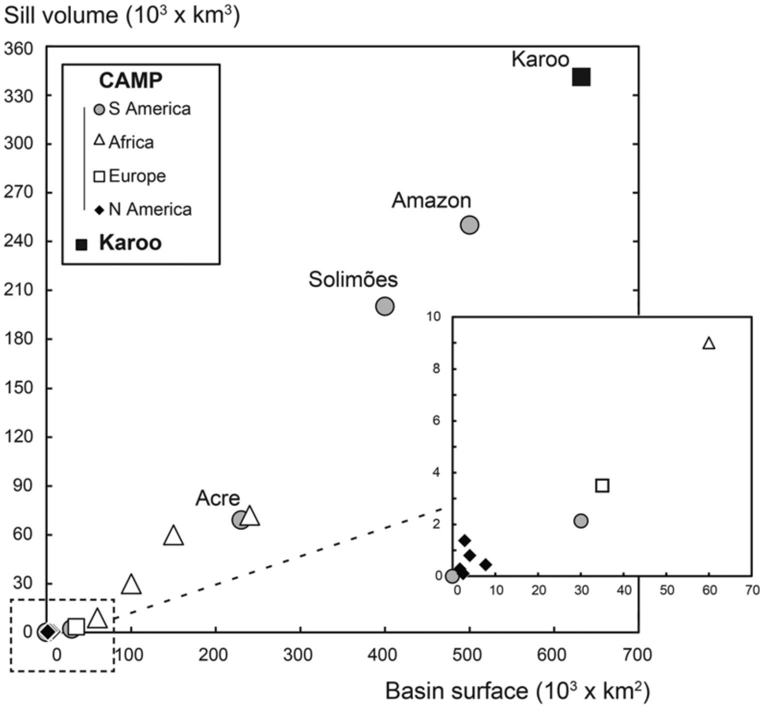

Fig. 6. The average volume of CAMP sills (in km^3) is plotted against the surface (in km^2) of the basins hosting them. Besides a clear positive correlation between the basin surface and total volume of the sills emplaced, the bigger volume of CAMP sills from the Brazilian basins compared to those from African, North American and European basins is visible. The inset is an enlarged detail of the smaller sills, and the volume of the Karoo sills is plotted for comparison.

aeolian sandstones, are locally present. A basaltic agglomerate, the Blackfell Rockhole Member, has been described as an explosive phreatomagmatic tephra deposit but was recently reinterpreted as 25–40 m-thick rubbly pahoehoe lava flow (Marshall *et al.* 2016). In the Antrim Plateau, the extrusive pile was emplaced above Proterozoic clastic sedimentary basins, and is overlain by stromatolitic limestones of Late Cambrian age.

Subvolcanic complexes and the igneous plumbing systems are poorly exposed. An eruptive centre in the central part of the Antrim Plateau has been proposed by Glass & Phillips (2006). The Milliwindi dolerite dyke, a NW-trending, more than 200 - km-long intrusion in the NW Kimberly, has also been proposed as a potential feeder dyke for the extrusive basalts (Hanley & Wingate 2000).

An extensive Early Cambrian intrusive complex is present in the Officer Basin in central Australia (Jourdan *et al.* 2014). This Neoproterozoic intracratonic basin is more than 8 km deep with an areal extent of more than 300 000 km^2. It is filled with marine carbonates, clastic sediments and evaporites. The structuring of the basin is mainly due to halokinesis. Dolerite sills are exposed in the NW Akubra-Boondawari area, and are penetrated by several petroleum exploration boreholes (Grey *et al.* 2005). Exploratory fieldwork in the Antrim Plateau region to the north revealed no presence of intrusive sills or hydrothermal vent complexes in the Proterozoic basins stratigraphically below the basalts.

A U–Pb zircon age of 510.7 ± 0.6 Ma obtained from the coarse-grained Milliwindi dolerite dyke is considered a minimum age for the onset of magmatic activity in the Kalkarindji LIP (Jourdan *et al.* 2014). This age overlaps the Early–Middle Cambrian boundary (510.0 ± 1.0 Ma: Landing *et al.* 1998; Harvey *et al.* 2011) and the associated extinction event (Fig. 4). The four $^{40}Ar/^{39}Ar$ ages that exist from the Kalkarindji LIP come from three flows and a sill, and range from 509.0 ± 2.6 to 511.9 ± 1.9 Ma, consistent with the U–Pb age (Glass & Phillips 2006; Evins *et al.* 2009; Jourdan *et al.* 2014).

The Central Atlantic Magmatic Province

Pangea was straddling the equator in the Late Triassic (Fig. 3), and the Central Atlantic Magmatic

Fig. 7. (**a**) Two lava flows in a small quarry in Kalkarindji LIP, Australia. Photograph: S. Planke. (**b**) Planar sills in the Nico Malan Pass road section in the Karoo Basin, South Africa. Photograph: H. H. Svensen. (**c**) CAMP lava flows emplaced in a Mesozoic sedimentary basin crop out near Aouli village (close to Midelt) in the Moroccan Middle Atlas. Photograph: S. Callegaro. (**d**) Thick sill intrusion into aeolian sandstones, NW Namibia, Etendeka. Photograph: D.A. Jerram. (**e**) Panoramic view of a thick lava sequence south of the Huab River, NW Namibia. Section length is approximately 7 km, Etendeka. Photograph: D.A. Jerram. (**f**) Panorama of thick dolerite sills around 'Finger Mountain', Trans-Antartic Mountains, Antarctica. Outcrop length is approximately 6 km. Photograph: D.A. Jerram.

Province (CAMP) magmatic activity was located at equatorial–subtropical latitudes. As for many other LIPs, CAMP assisted a major plate tectonic reorganization that led to the opening of the central part of the Atlantic Ocean at around 195 Ma, and thus split the main area of the supercontinent into northern and southern Pangea, with the latter again often termed Gondwana. With a north–south extension exceeding 6000 km and laterally spread along more than 2500 km, CAMP is thus preserved (Marzoli *et al.*

1999*b*) on the eastern margin of North America (from Nova Scotia to Florida), western Europe (France and Iberian Peninsula), in West Africa (from Morocco to the Ivory Coast) and northern South America (French Guyana, Surinam, Brazil, and Bolivia). CAMP magmatism is expressed by lava flows from fissure eruptions fed by dykes and sills, with magma ponding in deep and shallow magma chambers, a few of which are preserved to date as layered mafic intrusions.

Most of the CAMP rocks are tholeiitic low-Ti ($TiO_2 < 2$ wt%: De Min *et al.* 2003) continental flood basalts or basaltic andesites, whereas CAMP high-Ti tholeiites are restricted to a narrow zone in NE South America (Suriname, French Guyana and northern Brazil: Deckart *et al.* 2005; Merle *et al.* 2011) and the southern margin of the West African craton (Liberia, Sierra Leone). A peculiar feature of this LIP compared to what is observed for others is the lack of alkaline and acidic magmatism (cf. e.g. Karoo or Deccan Traps; Marsh & Eales 1984; Parisio *et al.* 2016) and the very minor volume of high-Ti products (cf., e.g., magmatism of the Paraná–Etendeka LIP: Peate & Hawkesworth 1996). CAMP lava piles are mainly preserved within continental Mesozoic rift basins, often filled with red beds and evaporites. Lava-flow remnants crop out interdigitated among (or are buried between) fluvio-lacustrine sediments in basins of the Newark Supergroup in the eastern USA and Nova Scotia (Merle *et al.* 2014), of the High and Middle Atlas, Arganà and Meseta in Morocco (Knight *et al.* 2004), and the Algarve and Santiago do Caçem in Portugal (Callegaro *et al.* 2014). The volcanic piles may range in overall thicknesses between 50 and 600 m (e.g. Merle *et al.* 2014). Notably, other smaller basins spread all over the surface of the province do contain minor volumes of lava flows, such as in Bolivia (Bertrand *et al.* 2014) or in Algeria (Béchar: Charaf Chabou *et al.* 2010). Erosion wiped away a large portion of the outpoured tholeiites, but since geochemical observations show that CAMP lava piles were fed by the preserved coeval dykes (e.g. McHone 1996; Puffer *et al.* 2009; Merle *et al.* 2014), the original surface of CAMP lava fields may have corresponded to that presently enclosed by the dyke swarms (McHone 2003).

From the assessment presented here, we estimate that the total volume of CAMP products ranges within 1×10^6–1.6×10^6 km^3. It is clear from this analysis that the Brazilian basins host the majority of CAMP products, both in terms of sills (520 000 km^3, *c.* 70% of the total volume of CAMP sills) and of lava flows (64 000 km^3, *c.* 40% of the total volume estimated for basinal extrusive products). This assessment further highlights the fact that an important portion of the CAMP is constituted by intrusive and subvolcanic products, and that the majority of them are hosted by organic-rich sedimentary basins. Detailed studies of the magma–sediment interaction, coupled with high-precision U–Pb geochronology, will be the key for understanding the impact of CAMP on the global climate.

Only two high-precision zircon U–Pb CA-ID-TIMS studies have been published for the CAMP (Fig. 4) (Schoene *et al.* 2010; Blackburn *et al.* 2013). In addition, three air abrasion multigrain zircon and/or baddeleyite U–Pb ID-TIMS studies from two sills and one basalt in North America had previously been published (Dunning & Hodych 1990; Hodych & Dunning 1992; Schoene *et al.* 2006). Due to much larger uncertainties or unconstrained Pb-loss, these data are not included in Figure 4. The oldest U–Pb-dated CAMP basalt (the North Mountain Basalt; lowermost flow in the Fundy Basin) from North America has an age of 201.566 ± 0.061–201.52 ± 0.14 Ma (two different samples: Blackburn *et al.* 2013) or 201.38 ± 0.22 Ma (Schoene *et al.* 2010), and ages range up to 201.274 ± 0.062 for the youngest dated basalt (Blackburn *et al.* 2013). Three sills are also dated from the North American part of CAMP, giving ages between 201.515 ± 0.062 and 200.916 ± 0.075 Ma, the latter being the youngest CAMP sample dated (Blackburn *et al.* 2013). One sill from Morocco, representing the only high-precision U–Pb date from the African part of the CAMP, is dated at 201.564 ± 0.075 Ma (Blackburn *et al.* 2013). Blackburn *et al.* (2013) estimated the end-Triassic extinction to have occurred at 201.564 ± 0.055 Ma, demonstrating synchronicity between early CAMP magmatism and extinction. Available $^{40}Ar/^{39}Ar$ ages show a relatively large range from *c.* 204 to *c.* 192 Ma, but with a significant majority clustering tightly around 201–202 Ma, also indistinguishable from the mean age of all CAMP magmatism (Marzoli *et al.* 2011).

The Karoo–Ferrar Large Igneous Province and related basins

The bulk of Pangea was still rather intact by the Early Jurassic, with limited opening of the Central Atlantic. Karoo–Ferrar magmatic activity in southern Gondwana was centred on southerly latitudes (30–60°S: Fig. 3). The Karoo–Ferrar LIP covers a vast range of Gondwanaland areas. It is extensively preserved throughout southern Africa (e.g. South Africa, Namibia and Lesotho: du Toit 1920; Marsh *et al.* 1997; Neumann *et al.* 2011), in Tasmania and in Antarctica (e.g. Heimann *et al.* 1994; White *et al.* 2009). Invariably, the intrusive component of this LIP is emplaced within thick sedimentary sequences (e.g. the Karoo Supergroup in Africa and the Beacon Supergroup in Antarctica). In both the Antarctica sections and the Karoo sequences, the sill complexes can be mapped from the basement up through the main sedimentary succession (e.g. du Toit 1920; Marsh & Eales 1984; Galerne *et al.* 2008; Polteau *et al.* 2008; Jerram *et al.* 2010; Svensen *et al.* 2015*b*). By far, the most extensively studied parts of the Karoo–Ferrar LIP are in the Southern African portion and this provides us with an extensive geochronological framework expanded on below.

The Upper Carboniferous–Jurassic Karoo Supergroup in South Africa has a maximum cumulative thickness of 12 km and a preserved maximum thickness of 5.5 km (Tankard *et al.* 2009). The current area with Karoo sediments cropping out in South Africa is about 630 000 km^2 (Svensen *et al.* 2015*b*). The depositional environments range from marine to fluvial and, finally, aeolian (Catuneanu *et al.* 1998). The Karoo Basin is overlain by 1.3 km of volcanic rocks of the Drakensberg Group, consisting mainly of stacked basalt flows erupted into a continental and dry environment. The plumbing system of the flood basalts is a basin-scale sill complex consisting of sills and dykes (Marsh & Eales 1984; Chevallier & Woodford 1999). The thickest sill in the basin is about 220 m thick, most are in the 10–60 m range, and the sills were emplaced at about 182.6 Ma (Svensen *et al.* 2012, 2015*c*). The composition of the sills is mainly tholeitic, with a few more evolved intrusions (andesitic) (Marsh & Eales 1984; Neumann *et al.* 2011).

Hundreds of breccia pipes and hydrothermal vent complexes are rooted in the contact aureoles in the Karoo Basin (Svensen *et al.* 2006, 2007). Alexander du Toit suggested that these degassing pipes formed due to igneous gas release, but recent research has stressed the importance of sediment-derived volatiles in their generation (e.g. Jamtveit *et al.* 2004; Svensen *et al.* 2007; Aarnes *et al.* 2010, 2012). The devolatilization involved both organic and inorganic reactions, leading to the formation of high-temperature minerals and lowering of the organic carbon content in shales (Aarnes *et al.* 2012; Svensen *et al.* 2015*b*). The hydrothermal vent complexes commonly crop out in the uppermost 400–500 m of the basin, and are associated with sills in the subsurface (Svensen *et al.* 2006, 2015*b*). In the upper parts of the basin stratigraphy (e.g. in the Elliot and Clarens formations), magma–water interactions led to the formation of phreatomagmatic complexes. One of the best-studied complexes, the Sterkspruit Complex, represents a >45 km^2 explosion crater filled with a variety of lavas, tuffs, sediment breccias, hyaloclastites and various other pyroclastic rocks (McClintock *et al.* 2008).

In Antarctica, the volcanic and subvolcanic rocks are scattered across vast areas along the Transantarctic Mountains and Queen Maud Land (e.g. Elliot & Fleming 2000; Elliot & Hanson 2001; McClintock & White 2006; White *et al.* 2009; Muirhead *et al.* 2014). Along the Transantarctic Mountains, a large sedimentary basin and its basement are exposed (e.g. Barrett *et al.* 1986; Storey *et al.* 2013). The sedimentary rocks are classified as the Beacon Supergroup and include Devonian–Triassic clastic sediments, mainly sandstones, also including Permian coal seams. Early Jurassic sedimentary rocks include sandstones intermixed and interbedded with tuffs and peperites (e.g. McClintock & White 2006; Muirhead *et al.* 2014). One of the most prominent sills in the Ferrar is the Peneplain sill, estimated to cover 19 000 km^2 with a thickness of 250 m (4750 km^3) (Gunn & Warren 1962; White *et al.* 2009). Other thick sills include the Basement sill and the Asgard and Mount Fleming sills, all of which attain thickness in the hundreds of metres and have a large aerial extent (e.g. Marsh 2004; Jerram *et al.* 2010).

There are three high-precision U–Pb ID-TIMS papers published from Karoo (Svensen *et al.* 2012; Sell *et al.* 2014; Burgess *et al.* 2015) and one extensive study from Ferrar (including 19 samples from three different areas of Antarctica and one sample from Tasmania: Burgess *et al.* 2015) (Fig. 4). The ages from Karoo obtained by Svensen *et al.* (2012) were mainly obtained on air-abraded zircons, with only a few chemically abraded zircons, but the study includes an extensive dataset on 14 samples with concordant zircons showing a large degree of consistency and, thus, most probably representing the true ages of the dated sills within uncertainty. The zircon ages from Sell *et al.* (2014) and Burgess *et al.* (2015) were obtained by CA-ID-TIMS. Only sills have been dated from Karoo and the ages range from 183.4 ± 0.4 to 182.7 ± 0.6 Ma (Svensen *et al.* 2012; Corfu *et al.* 2016), with the two most precise ages being 183.246 ± 0.066 and 183.014 ± 0.075 Ma (Sell *et al.* 2014; Burgess *et al.* 2015). In Ferrar, 20 samples from 10 lavas, eight sills and two intrusions have been dated by CA-ID-TIMS (Burgess *et al.* 2015). The lava ages range from 182.779 ± 0.066 to 182.430 ± 0.066 Ma, and the intrusive rocks range in age from 182.85 ± 0.35 to 182.540 ± 0.075 Ma (Burgess *et al.* 2015). Different astrochronological models exist for the onset of the Toarcian Ocean Anoxic Event (TOAE), one model placing the onset of the TOAE at 183.1 Ma (Boulila *et al.* 2014) and another at 182.75 Ma (Suan *et al.* 2008; Burgess *et al.* 2015), both anchored at the radiometrically determined Pliensbachian–Toarcian boundary age of $183.6 + 1.7/-1.1$ (Pálfy *et al.* 2000; Sell *et al.* 2014). Whichever model is used, magmatism in Karoo overlaps the TOAE, while magmatism in Ferrar only overlaps with the TOAE using the model of Suan *et al.* (2008). Sills and lavas dated by $^{40}Ar/^{39}Ar$ show a relatively large spread (Fig. 4), but the majority of ages cluster between *c.* 182 and 186 Ma (Jourdan *et al.* 2008).

Paraná–Etendeka

By the Early Cretaceous, seafloor spreading in the Central Atlantic and the West Somali and Mozambique basins were well under way. The continents were spread from pole-to-pole and Paraná–Etendeka erupted at southerly subtropical latitudes (Fig. 3). The Cretaceous break-up of South America from Africa is a late-stage part of the Gondwana break-up and the Paraná–Etendeka LIP is the manifestation of this break-up; plume activity with volcanism started at 135–134 Ma, with large volumes of magma occurring in the first few million years up to, and including, the onset of break-up (e.g. Jerram & Widdowson 2005). This volcanism and the pre-volcanic stratigraphy help to correlate the Paraná (Brazil) with the Etendeka (Namibia). A large volume of the preserved volcanic rocks are found on the Paraná side.

The volcanic stratigraphy of the Paraná–Etendeka, as for many of the LIPs, has been mapped on a gross scale using chemostratigraphic relationships (e.g. Paraná: Peate 1997; Etendeka: Marsh *et al.* 2001). Increasingly detailed field-based volcanological correlations of the lava sequences have also identified disconformities within lava sequences of the same chemostratigraphic type, as well as detailed understanding of the volcanic evolution of the province (e.g. Jerram *et al.* 1999; Jerram & Stollhofen 2002; Waichel *et al.* 2008). Also, key correlations with the base basalt sequences and the immediate underlying and interbedded stratigraphy (Jerram & Widdowson 2005; Petry *et al.* 2007; Waichel *et al.* 2012) have been made. Correlations across the South Atlantic are possible using these stratigraphic and chemical relationships between key units. Volumes calculated with help from these correlations highlight large-volume individual events, with some of the largest individual silicic eruptions adding up to several thousands of km^3 (Bryan *et al.* 2010). Such events are manifested as both eruptions and as intrusions with big sill and volcanic centre complexes (Jerram & Bryan 2015).

The Paraná–Etendeka has also been linked with climatic changes as recorded by carbon isotope excursions, specifically the mid-Valanginian Weissert Event (e.g. Erba *et al.* 2004; Aguirre-Urreta *et al.* 2015; Martinez *et al.* 2015). However, the scale and impact of this event is somewhat small compared to events such as the end-Permian. The volcanic basin of the Paraná–Etendeka contains significant aeoilan deposits (Mountney *et al.* 1998; Jerram *et al.* 2000), and great interaction of the volcanics with these sandstones is observed (Jerram & Stollhofen 2002; Petry *et al.* 2007). As such, there may have been a dampening down of the effects of gasses given off during this event compared to other LIPs as the interaction can often result in a net sequestration of gasses, such as CO_2 in diagenetic cements (Jones *et al.* 2016).

The geochronological picture from the Paraná–Etendeka is incomplete. Some U–Pb ID-TIMS age data include a combined zircon (multigrain fraction; air abraded) and baddeleyite (multigrain) weighted mean age from a dacitic volcanic rock (Janasi *et al.* 2011), and a five-zircon (multigrain; CA) upper intercept age from a composite dyke (Florisbal *et al.* 2014). No tracer calibration uncertainties were reported for these data but, as the uncertainties on the calculated ages are rather large, this is not a critical factor for comparison with other ages. The interpreted ages for the dacite and the dyke, respectively, are 134.3 ± 0.8 and 133.9 ± 0.7 Ma (Janasi *et al.* 2011; Florisbal *et al.* 2014), but due to the number few analyses and the clear presence of Pb loss in the analysed zircons, the accuracy of the ages cannot be considered as highly robust. Thiede & Vasconcelos (2010) reviewed $^{40}Ar/^{39}Ar$ ages from the Paraná and compiled the most robust ages. They also re-analysed some of the samples that deviated significantly from the mean age, and showed that all robust ages cluster tightly and define an interval of magmatism of less than *c.* 1.2 Ma, with a mean age of 134.6 Ma. Recent palaeomagnetic data suggest a longer lived magmatic range of *c.* 4 Ma, within a similar time frame (Dodd *et al.* 2015).

On the Etendeka (Namibian) side, there are only $^{40}Ar/^{39}Ar$ ages reported (e.g. Renne *et al.* 1996; Jerram *et al.* 1999; Marzoli *et al.* 1999*a*). They are stated as slightly younger (133–132 Ma) but when recalculated using the latest techniques for Ar/Ar calibration (Kuiper *et al.* 2008; Renne *et al.* 2010, see also Dodd *et al.* 2015), these come in at *c.* 134 Ma, overlapping with ages from the Paraná Basin (Fig. 4). Magmatic activity in the Paraná–Etendeka Magmatic Province appears to be slightly younger – but overlapping within error – than the onset of the mid-Valanginian Weissert Event (carbon isotope shift), dated at 135.22 ± 1.0 Ma (e.g. Aguirre-Urreta *et al.* 2015; Martinez *et al.* 2015). The question of synchronicity and matching between the geochronological data available for the two events remains open until better age constraints are attained.

LIPs, plates and the big picture

The dawn of the Phanerozoic is exceptional in many ways: most continents were located in the southern hemisphere, the atmospheric CO_2 concentration was, perhaps, 5–10 times the current level, and a global sea-level rise with largely warm surface seawater temperatures appear to have characterized the Cambrian and much of the Ordovician (Fig. 8). Abrupt changes in the atmospheric concentration of greenhouse gases have occurred episodically through Earth's history, and many of these climatic and environmental perturbations show a causal relationship with LIP eruptions, which have been sourced by plumes from the margins of two main thermochemical provinces in the deep mantle, TUZO and JASON. The Gondwana LIPs were all sourced from TUZO (Figs 2 & 3). During the Palaeozoic, most of the continents moved northwards, Pangea formed in the Late Carboniferous, and by the Late Triassic Pangea was centred around the equator and overlying the TUZO LLSVP (Fig. 3). CAMP magmatic activity was located to equatorial–subtropical latitudes, and contemporaneous kimberlites are found in southern Africa and North America. CAMP and kimberlites were sourced by deep plumes from the western margin of TUZO. The CAMP marks the initial break-up of the Pangaea supercontinent, relicts of its extensive tholeiitic magmatism are presently preserved in four continents along both sides of the Atlantic Ocean (Marzoli *et al.* 1999*b*), and CAMP contributed to one of the 'big five' biotic extinction events in the Phanerozoic.

By the Early Cretaceous, seafloor spreading in the Central Atlantic and the West Somali and Mozambique basins were well underway. The continents were spread from pole-to-pole and Paraná–Etendeka erupted at southerly subtropical latitudes (Fig. 3) with contemporaneous kimberlite activity in South Africa, Namibia and NW Africa. As for the end-Triassic and Early Jurassic, this magmatic activity was sourced by deep plumes along the western margin of TUZO. This is also exemplified in Figure 9: in this schematic cartoon we envisage that long-lived subduction along the South American (Andean) margin was the triggering mechanism for a deep plume that eventually rose through the mantle and led to catastrophic upper mantle melting, forming the Paraná–Etendeka LIP.

LIPs may have caused or contributed to four of the 'big five' biotic extinction events in the Phanerozoic: the end-Devonian (Yakutsk in Siberia), the end-Permian (Siberian Traps), the end-Triassic (Central Atlantic Magmatic Province, CAMP) and the end-Cretaceous (K-Pg: Deccan Traps). In addition, the Middle Permian extinction (Capitanian) was causally linked to the Emeishan LIP (e.g. Bond *et al.* 2010; Jerram *et al.* 2016*b*), but formed outside Gondwana and is thus not included in this work. The K-Pg mass extinction event, however, is unique because it is coincident with the Chicxulub bolide impact. The oldest Phanerozoic extinction, and the third in importance, at the end of the Ordovician (Hirnantian) is not linked with any known LIP, even though widespread explosive volcanism is suggested to have played a role in the global cooling (Buggisch *et al.* 2010).

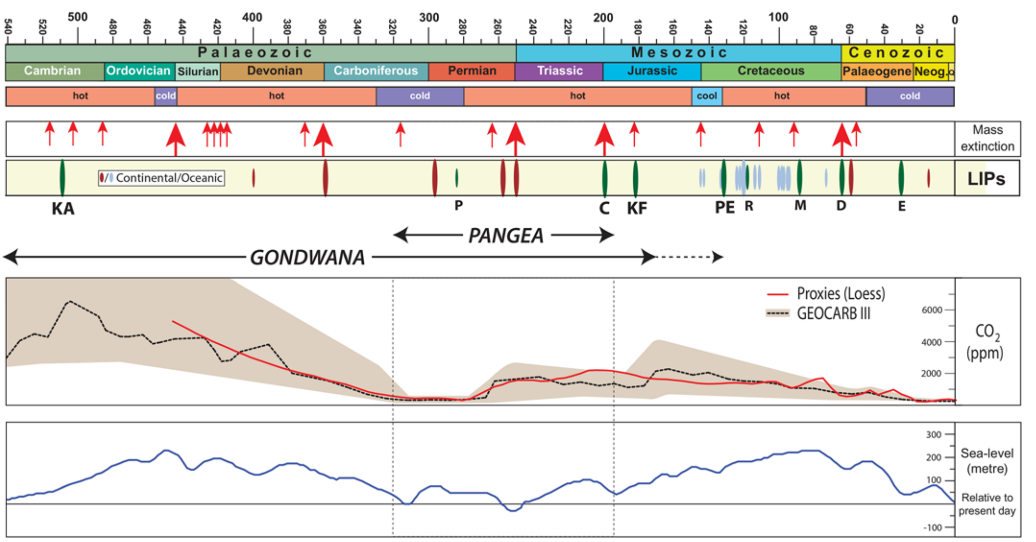

Fig. 8. Phanerozoic timescale, icehouse (cold) v. greenhouse (hot) conditions, extinction events (five major with larger arrows), global LIP events (continental and oceanic), atmospheric p_{CO_2} (Royer 2006) and global sea-level variations (Haq & Al-Qahtani 2005; Haq & Shutter 2008). Abbreviations for LIPs affecting Gondwana continental lithosphere are as follows: KA, Kalkarindji; P, Panjal; C, Central Atlantic Magmatic Province; KF, Karoo-Ferrar; PE, Parená-Etendeka; R, Rajhmahal; M, Madagascar; D, Deccan; E, Ethiopia. We have also indicated with arrows the life time of Gondwana and Pangea.

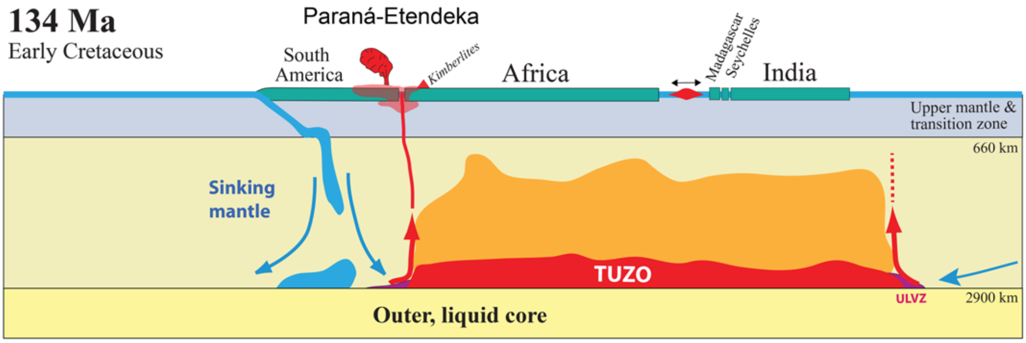

Fig. 9. Subducted lithospheric slabs may interact with the margins of TUZO and JASON, triggering the formation of plumes. The cartoon is a profile approximately through the reconstructed Paraná–Etendeka LIP, North Madagascar–Seychelles and India (cf. Fig. 3) at around 135 Ma. The triggering slabs for plumes sourcing the Paraná–Etendeka LIP and contemporaneous kimberlites in South Africa and Namibia must clearly have been linked to subduction along the western margin of South America. The South Atlantic opened shortly after the Paraná–Etendeka LIP.

The importance of subvolcanic intrusions and sill volumes

The timing of environmental changes and LIPs is summarized in Figure 8. Several processes are suggested as links between LIPs and environmental changes, including: (1) lava degassing of mantle volatiles, with or without a contribution from recycled continental crust; (2) degassing of volatiles derived from the sill-related contact aureoles of heated sedimentary rocks; and (3) degassing from sills and lavas contaminated by volatiles derived from the intruded sedimentary rocks or other crustal rocks (e.g. Svensen *et al.* 2004; Ganino & Arndt 2009; Sobolev *et al.* 2011). The actual extinction mechanisms are debated, and the suggestions include extreme temperatures, oceanic anoxia and pH reduction, sulphuric acid poisoning, and ozone layer destruction followed by extreme UV-B radiation (e.g. Visscher *et al.* 2004; Robock 2005; Bacon *et al.* 2013; Elliott-Kingston *et al.* 2014).

The importance of volcanic basins for the evolution of LIPs and the relationship to environmental changes has been stressed in recent years. During the formation of LIPs, magma is commonly emplaced as sills, dykes and igneous centres in the upper crust (Jerram & Bryan 2015). In cases where the volume of magma emplaced in sedimentary basins is high, these basins are commonly referred to as 'volcanic basins' (Fig. 10) (e.g. Jerram 2015; Abdelmalak *et al.* 2016; Jerram *et al.* 2016*a*). Volcanic basins are present along rifted continental margins and on lithospheric cratons (e.g. Coffin & Eldholm 1994), and represent vast basin areas that contain significant volumes of LIP-related igneous rocks and, in some cases, particularly where underplating has occurred and sill complexes exist, the intrusive component can be larger than the extrusive counterparts (basalt/lava) and pyroclastic deposits. Sill emplacement is characterized by the development of hydrothermal vent complexes that cut up through the basin and erupt at the surface through pipe structures (e.g. Fig. 10) (Svensen *et al.* 2006; Jerram *et al.* 2016*a*) that can be found both before and within the volcanic pile and which can indicate the relative timing of the sill emplacement (e.g. Angkasa *et al.* 2017).

Sill thicknesses can exceed 350 m, sandwiched between sedimentary sequences and associated contact metamorphic aureoles. Sills can also occur within the lava piles themselves (e.g. Hansen *et al.* 2011), but their identification is complicated within a similar host rock and also emphasizes a potential for the underestimate of the volume of the intrusive component. A selection of field photographs from several of the LIPs described in this work is shown in Figure 7. Contact metamorphism of the host sedimentary rocks cause devolatilization and the generation of H_2O, CO_2, CH_4 and SO_2 depending on the composition of the country rocks, including their content of organic carbon (e.g. Svensen *et al.* 2009). As a rule of thumb, the volume of heated sedimentary rocks is twice the sill volume, as suggested both by modelling studies and by mineral and maceral temperature proxies (e.g. Aarnes *et al.* 2011). These volatiles may reach the atmosphere via direct degassing in breccia pipes and hydrothermal vent complexes or by seepage through fractures and sediment permeability. In addition to the sediment degassing, basalt lava degassing releases a range of volatiles to the atmosphere, including CO_2 and SO_2 (e.g. Self *et al.* 2006).

A classic epitome of the LIP mass-extinction paradigm is the relationship between CAMP and end-Triassic mass extinction. Combined geochronological and stratigraphic data have evidenced that the

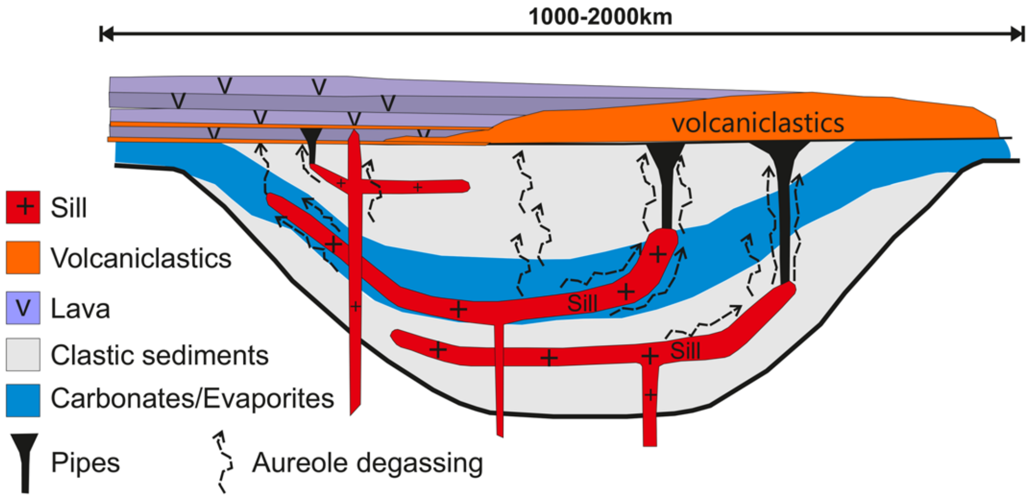

Fig. 10. Schematic cross-section of a volcanic basin, showing sills, dykes, pipes, and surface deposits of lava and pyroclastics. Modified from Jerram *et al.* (2016*a*).

two events coincide, but few constraints exist on how the CAMP played its forcing on the end-Triassic global environment. On the stratigraphic record, from worldwide localities, the end-Triassic biotic crisis is also associated to a negative carbon isotope excursion that reflects a disruption of the carbon cycle, for which the CAMP is considered the cause. Modelling shows that the sharp negative $\delta^{13}C$ excursion associated with the extinction can be obtained by rapid release of very isotopically light carbon (e.g. Bachan & Payne 2016). Since carbon released by flood basalt magmatism is isotopically too heavy to drive such negative excursions, the source of isotopically light carbon must be sought in the degassing from heated sediments. In this view, the study of subvolcanic intrusions and the estimation of sill volumes are fundamental because the degassing from organic-rich sediments in contact with such magmatic structures is, to the best of our knowledge, the most efficient way to transfer volatiles from the lithosphere to the Earth's atmosphere during LIP events. The volume estimation of CAMP magmas presented here further highlights that an important portion of the CAMP is constituted by intrusive and subvolcanic products, and that the majority of them are hosted by the organic-rich sedimentary basins in Brazil.

There are still unresolved aspects related to the age of sills and dykes, their volumes, and emplacement rate, even though recent work has made advances in several LIPs (e.g. Jourdan *et al.* 2005, 2014; Svensen *et al.* 2012; Blackburn *et al.* 2013; Burgess *et al.* 2015). These issues are challenging to resolve as sills and dykes are non-uniformly distributed in volcanic basins, and basin-scale 3D seismic data and boreholes are not always available. Still, we stress that current knowledge and data suggest that the subvolcanic intrusions in sedimentary basins hold a key to understand past environmental changes.

Summary

- In Palaeozoic and Early Mesozoic times, Gondwana LIPs and the majority of kimberlites were sourced by deep plumes from the margins of the African LLSVP (TUZO), one of two major stable thermochemical piles at the core–mantle boundary. Gondwana essentially existed from Cambrian to Jurassic times and in its lifetime three continental LIPs (Kalkarindji, CAMP and Karoo–Ferrar) directly affected Gondwanan continental crust at around 510, 201 and 183 Ma.
- Two of these LIPs (CAMP and Karoo–Ferrar) assisted the break-up of Gondwana and Pangea, as witnessed by the opening of the Central Atlantic Ocean (splitting Pangea) and the West Somali and Mozambique basins (separating West and East Gondwana) during the Jurassic.
- Soon after, the opening of the South Atlantic in the early Cretaceous from around 130 Ma took place only about 4–5 myr from the onset of the Paraná–Etendeka LIP, which affected vast areas in Brazil and parts of Namibia.
- The architecture of the major Gondwana LIPs consists of a subvolcanic and a volcanic part. Subvolcanic sills and dykes represent a significant part of the LIP igneous volume, commonly emplaced in sedimentary basins (i.e. volcanic

basins). Sills are commonly present throughout the basin stratigraphies and the sill volumes are thus scaled to the basin size.

- A new assessment of the CAMP LIP shows that the sills have a volume of about 700 000 km^3 (based on an average volume estimate – Table 3), more than half of it present in the Brazilian basins. This suggests that sill emplacement and the related contact metamorphism and devolatilization probably contributed to the climatic change and mass extinction at the end of the Triassic.

This work was supported by the Research Council of Norway through its Centres of Excellence funding scheme to the Centre of Earth Evolution and Dynamics (CEED), project number 223272. L. Parisio is thanked for fruitful insights and discussions over the extent of CAMP outcrops.

References

Aarnes, I., Svensen, H., Connolly, J.A.D. & Podladchikov, Y.Y. 2010. How contact metamorphism can trigger global climate changes: modeling gas generation around igneous sills in sedimentary basins. *Geochimica et Cosmochimica Acta*, **74**, 7179–7195.

Aarnes, I., Svensen, H., Polteau, S. & Planke, S. 2011. Contact metamorphic devolatilization of shales in the Karoo Basin, South Africa, and the effects of multiple sill intrusions. *Chemical Geology*, **281**, 181–194.

Aarnes, I., Podladchikov, Y. & Svensen, H. 2012. Devolatilization-induced pressure build-up: implications for reaction front movement and breccia pipe formation. *Geofluids*, **12**, 265–279, https://doi.org/10.1111/j.1468-8123.2012.00368.x

Abdelmalak, M.M., Planke, S., Faleide, J.I., Jerram, D. A., Zastrozhnov, D., Eide, S. & Myklebust, R. 2016. The development of volcanic sequences at rifted margins: new insights from the structure and morphology of the Vøring Escarpment, mid-Norwegian Margin. *Journal of Geophysical Research: Solid Earth*, **121**, 5212–5236, https://doi.org/10.1002/2015JB012788

Aguirre-Urreta, B., Lescano, M., Schmitz, M.D., Tunik, M., Concheyro, A., Rawson, P.F. & Ramos, V.A. 2015. Filling the gap: new precise Early Cretaceous radioisotopic ages from the Andes. *Geological Magazine*, **152**, 557–564.

Almeida, F.F.M. 1986. Distribuição regional e relações tectônicas do magmatismo pós-Palcozóico no Brasil. *Revista Brasileira de Geociências*., **16**, 325–349.

Angkasa, S.S., Jerram, D.A. *et al.* 2017. Mafic intrusions, hydrothermal venting, and the basalt-sediment transition: Linking onshore and offshore examples from the North Atlantic igneous Province. *Interpretation*, **5**, ISSN: 2324-8858, published 15 May 2017.

Bachan, A. & Payne, J.L. 2016. Modelling the impact of pulsed CAMP volcanism on p_{CO_2} and $\delta^{13}C$ across the Triassic–Jurassic transition. *Geological Magazine*, **153**, 252–270.

Bacon, K.L., Belcher, C.M., Haworth, M. & McElwain, J.C. 2013. Increased atmospheric SO_2 detected from changes in leaf physiognomy across the Triassic–Jurassic boundary interval of East Greenland. *PloS ONE*, **8**, e60614.

Barrett, P.J., Elliot, D.H. & Lindsay, J.F. 1986. The Beacon supergroup (Devonian–Triassic) and Ferrar Group (Jurassic) in the Beardmore glacier area, Antarctica. *Antarctic Research Series*, **36**, 339–428.

Bertrand, H., Fornari, M., Marzoli, A., García-Duarte, R. & Sempere, T. 2014. The Central Atlantic Magmatic Province extends into Bolivia. *Lithos*, **188**, 33–43.

Beutel, E.K., Nomade, S., Fronabarger, A.K. & Renne, P.R. 2005. Pangea's complex breakup: a new rapidly changing stress field model. *Earth and Planetary Science Letters*, **236**, 471, https://doi.org/10.1016/j.epsl.2005.03.021

Béziat, D., Joron, J.L., Monchoux, P., Treuil, M. & Walgenwitz, F. 1991. Geodynamic implications of geochemical data for the Pyrenean ophites (Spain–France). *Chemical Geology*, **89**, 243–262.

Blackburn, T.J., Olsen, P.E. *et al.* 2013. Zircon U–Pb geochronology links the end-Triassic extinction with the Central Atlantic Magmatic Province. *Science*, **340**, 941–945.

Bond, D.P.G., Hilton, J., Wignall, P.B., Ali, J.R., Stevens, L.G., Sun, Y.-D. & Lai, X.-L. 2010. The Middle Permian (Capitanian) mass extinction on land and in the oceans. *Earth-Science Reviews*, **102**, 100–116, https://doi.org/10.1016/j.earscirev.2010.07.004

Boulila, S., Galbrun, B., Huret, E., Hinnov, L., Rouget, I., Gardin, S. & Bartolini, A. 2014. Astronomical calibration of the Toarcian Stage: implications for sequence stratigraphy and duration of the early Toarcian OAE. *Earth and Planetary Science Letters*, **386**, 98–111.

Bryan, S.E., Ukstins Peate, I. *et al.* 2010. The largest volcanic eruptions on Earth. *Earth-Science Reviews*, **102**, 207–229.

Buggisch, W., Joachimski, M.M., Lehnert, O., Bergström, S.M., Repetski, J.E. & Webers, G.F. 2010. Did intense volcanism trigger the first late Ordovician icehouse? *Geology*, **38**, 327–330.

Burgess, S.D., Bowring, S.A., Fleming, T.H. & Elliot, D.H. 2015. High-precision geochronology links the Ferrar large igneous province with early-Jurassic ocean anoxia and biotic crisis. *Earth and Planetary Science Letters*, **415**, 90–99.

Burke, K., Steinberger, B., Torsvik, T.H. & Smethurst, M.A. 2008. Plume generation zones at the margins of large low shear velocity provinces on the core–mantle boundary. *Earth and Planetary Sciences*, **265**, 49–60.

Callegaro, S., Rapaille, C. *et al.* 2014. Enriched mantle source for the Central Atlantic magmatic province: new supporting evidence from southwestern Europe. *Lithos*, **188**, 15–32.

Catuneanu, O., Hancox, P.J. & Rubidge, B.S. 1998. Reciprocal flexural behaviour and contrasting stratigraphies: a new basin development model for the Karoo retroarc foreland system, South Africa. *Basin Research*, **10**, 417–439.

Charaf Chabou, M., Bertrand, H. & Sebaï, A. 2010. Journal of African Earth Sciences Geochemistry of the Central Atlantic Magmatic Province (CAMP) in south-western Algeria. *Journal of African Earth Sciences*, **58**, 211–219.

Chevallier, L. & Woodford, A. 1999. Morpho-tectonics and mechanism of emplacement of the dolerite rings and sills of the western Karoo, South Africa. *South African Journal of Geology*, **102**, 43–54.

COFFIN, M.F. & ELDHOLM, O. 1994. Large Ignoeus Provinces: crustal structure, dimensions and external consequences. *Reviews of Geophysics*, **32**, 1–36.

COHEN, K.M., FINNEY, S.C., GIBBARD, P.L. & FAN, J.-X. 2013. The ICS International Chronostratigraphic Chart. *Episodes*, **36**, 199–204.

CONDON, D.J., SCHOENE, B., MCLEAN, N.M., BOWRING, S.A. & PARRISH, R.R. 2015. Metrology and traceability of U–Pb isotope dilution geochronology (EARTHTIME Tracer Calibration Part I). *Geochimica et Cosmochimica Acta*, **164**, 464–480.

CORFU, F., SVENSEN, H. & MAZZINI, A. 2016. Comment to paper: evaluating the temporal link between the Karoo LIP and climatic–biologic events of the Toarcian Stage with high-precision U–Pb geochronology by Bryan Sell, Maria Ovtcharova, Jean Guex, Annachiara Bartolini, Fred Jourdan, Jorge E. Spangenberg, Jean-Claude Vicente, Urs Schaltegger in *Earth and Planetary Science Letters*, 408 (2014) 48–56. *Earth and Planetary Science Letters*, **434**, 349–352.

DECKART, K., BERTRAND, H. & LIÉGEOIS, J.-P. 2005. Geochemistry and Sr, Nd, Pb isotopic composition of the Central Atlantic Magmatic Province (CAMP) in Guyana and Guinea. *Lithos*, **82**, 289–314.

DE MIN, A., PICCIRILLO, E.M., MARZOLI, A., BELLIENI, G., RENNE, P.R., ERNESTO, M. & MARQUES, L.S. 2003. The Central Atlantic Magmatic Province (CAMP) in Brazil: petrology, geochemistry, $^{40}Ar/^{39}Ar$ ages, paleomagnetism and geodynamic implications. The central Atlantic magmatic province: insights from fragments of Pangea. *In*: HAMES, W., MCHONE, J.G., RENNE, P.C. & RUPPEL, C. (eds) *The Central Atlantic Magmatic Province: Insights from Fragments of Pangea*. American Geophysical Union, Geophysical Monograph Series, **136**, 91–128, https://doi.org/10.1029/136GM06

DODD, S.C., MAC NIOCAILL, C. & MUXWORTHYA, A.R. 2015. Long duration (>4 Ma) and steady-state volcanic activity in the early Cretaceous Paraná–Etendeka Large Igneous Province: new palaeomagnetic data from Namibia. *Earth and Planetary Science Letters*, **414**, 16–29.

DOUBROVINE, P.V., STEINBERGER, B. & TORSVIK, T.H. 2016. A failure to reject: testing the correlation between large igneous provinces and deep mantle structures with EDF statistics. *Geochemistry, Geophysics, Geosystems*, **17**, 1130–1163, https://doi.org/10.1002/2015GC006044

DUNNING, G.R. & HODYCH, J.P. 1990. U/Pb zircon and baddeleyite ages for the Palisades and Gettysburg sills of the northeastern United States: implications for the age of the Triassic/Jurassic boundary. *Geology*, **18**, 795, https://doi.org/10.1130/0091-7613(1990)0182.3.CO;2

DU TOIT, A.I. 1920. The Karoo dolerites of South Africa: a study in hypabyssal injection. *Transactions of the Geological Society of South Africa*, **23**, 1–42.

ELLIOT, D.H. & FLEMING, T.H. 2000. Weddell triple junction: the principal focus of Ferrar and Karoo magmatism during initial breakup of Gondwana. *Geology*, **28**, 539–542.

ELLIOT, D.H. & HANSON, R.E. 2001. Origin of widespread, exceptionally thick basaltic phreatomagmatic tuff breccia in the Middle Jurassic Prebble and Mawson Formations, Antarctica. *Journal of Volcanology and Geothermal Research*, **111**, 183–201.

ELLIOTT-KINGSTON, C., HAWORTH, M. & MCELWAIN, J.C. 2014. Damage structures in leaf epidermis and cuticle as an indicator of elevated atmospheric sulphur dioxide in early Mesozoic floras. *Review of Palaeobotany and Palynology*, **208**, 25–42.

ERBA, E., BARTOLINI, A. & LARSON, R.L. 2004. Valanginian Weissert oceanic anoxic event. *Geology*, **32**, 149–152.

ERNST, R.E. 2014. *Large Igneous Provinces*. Cambridge University Press, London.

EVINS, L., JOURDAN, F. & PHILIPS, D. 2009. The Cambrian Kalkarindji Large Igneous Province: extent and characteristics based on new $^{40}Ar/^{39}Ar$ and geochemical data. *Lithos*, **110**, 294–304, https://doi.org/10.1016/j.lithos.2009.01.014

FLORISBAL, L.M., HEAMAN, L.M., DE ASSIS JANASI, V.A. & DE FATIMA BITENCOURT, M. 2014. Tectonic significance of the Florianópolis dyke Swarm, Paraná–Etendeka Magmatic Province: a reappraisal based on precise U–Pb dating. *Journal of Volcanology and Geothermal Research*, **289**, 140–150.

FRANK, H.T., ELISA, M., GOMES, B., LUIZ, M. & FORMOSO, L. 2009. Review of the areal extent and the volume of the Serra Geral Formation, Paraná Basin, South America. *Pesquisas em Geosciences*, **36**, 49–57.

GALERNE, C.Y., NEUMANN, E.R. & PLANKE, S. 2008. Emplacement mechanisms of sill complexes: information from the geochemical architecture of the Golden Valley Sill Complex, South Africa. *Journal of Volcanology and Geothermal Research*, **177**, 425–440.

GANINO, C. & ARNDT, N.T. 2009. Climate changes caused by degassing of sediments during the emplacement of large igneous provinces. *Geology*, **37**, 323–326.

GLASS, L.M. & PHILLIPS, D. 2006. The Kalkarindji continental flood basalt province: a new Cambrian large igneous province in Australia with possible links to faunal extinctions. *Geology*, **34**, 461–464, https://doi.org/10.1130/G22122.1

GREY, K., HOCKING, R.M. ET AL. 2005. *Lithostratigraphic Nomenclature of the Officer Basin and Correlative Parts of the Paterson Orogen Western Australia*. Geological Survey of Western Australia, Report 93.

GUNN, B.M. & WARREN, G. 1962. Geology of Victoria Land between the Mawson and Murlock Glaciers, Antarctica. *New Zealand Geological Survey Bulletin*, **71**, 1–157.

HAMES, W.E., RENNE, P.R. & RUPPEL, C. 2000. New evidence for geologically instantaneous emplacement of earliest Jurassic Central Atlantic magmatic province basalts on the North 7 American margin. *Geology*, **28**, 859, https://doi.org/10.1130/0091-7613(2000)282.0.CO;2

HANLEY, L.M. & WINGATE, M.T.D. 2000. SHRIMP zircon age for an Early Cambrian dolerite dyke: an intrusive phase of the Antrim Plateau Volcanics of northern Australia. *Australian Journal of Earth Sciences*, **47**, 1029–1040, https://doi.org/10.1046/j.1440-0952.2000.00829.x

HANSEN, J., JERRAM, D.A., MCCAFFREY, K. & PASSEY, S.R. 2011. Early Cenozoic saucer-shaped sills of the Faroe Islands: an example of intrusive styles in basaltic lava piles. *Journal of the Geological Society, London*, **168**, 159–178, https://doi.org/10.1144/0016-7649 2010-012

HAQ, B.U. & AL-QAHTANI, A.M. 2005. Phanerozoic cycles of sea-level change on the Arabian Platform. *GeoArabia*, **10**, 127–160.

HAQ, B.U. & SHUTTER, S.R. 2008. A chronology of Paleozoic sea-level changes. *Science*, **322**, 64–68.

HARVEY, T.H.P., WILLIAMS, M. *ET AL.* 2011. A refined chronology for the Cambrian succession of southern Britain. *Journal of the Geological Society, London*, **168**, 705–716, https://doi.org/10.1144/0016-76492010-031

HEIMANN, A., FLEMING, T.H., ELLIOT, D.H. & FOLAND, K.A. 1994. A short interval of Jurassic continental flood basalt volcanism in Antarctica as demonstrated by $^{40}Ar/^{39}Ar$ geochronology. *Earth and Planetary Science Letters*, **121**, 19–41.

HODYCH, J.P. & DUNNING, G.R. 1992. Did the Manicouagan impact trigger end-of-Triassic mass extinction? *Geology*, **20**, 51–54, https://doi.org/10.1130/0091-7613(1992)0202.3.CO;2

JAMTVEIT, B., SVENSEN, H., PODLADCHIKOV, Y. & PLANKE, S. 2004. Hydrothermal vent complexes associated with sill intrusions in sedimentary basins. *In*: BREITKREUZ, C. & PETFORD, N. (eds) *Physical Geology of High-Level Magmatic Systems*. Geological Society, London, Special Publications, **234**, 233–241, https://doi.org/10.1144/GSL.SP.2004.234.01.15

JANASI, V.A., DE FREITAS, V.A. & HEAMAN, L.H. 2011. The onset of flood basalt volcanism, Northern Paraná Basin, Brazil: a precise U–Pb baddeleyite/zircon age for a Chapecótype dacite. *Earth and Planetary Science Letters*, **302**, 147–153.

JERRAM, D.A. 2015. *Hot Rocks and Oil: Are Volcanic Margins the New Frontier?* Geofacets. Elsevier, Amsterdam, https://www.elsevier.com/__data/assets/pdf_file/0008/84887/ELS_Geofacets-Volcanic-Article_Digital_r5.pdf

JERRAM, D.A. & BRYAN, S.E. 2015. Plumbing systems of shallow level intrusive complexes. *In*: BREITKREUZ, C. & ROCCHI, S. (eds) *Physical Geology of Shallow Magmatic Systems*. ISBN: 978-3-319-14083-4. Springer International Publishing.

JERRAM, D.A. & STOLLHOFEN, H. 2002. Lava/sediment interaction in desert settings; are all peperite-like textures the result of magma–water interaction? *Journal of Volcanology and Geothermal Research*, **114**, 231–249.

JERRAM, D.A. & WIDDOWSON, M. 2005. The anatomy of Continental Flood Basalt Provinces: geological constraints on the processes and products of flood volcanism. *Lithos*, **79**, 385–405.

JERRAM, D.A., MOUNTNEY, N., HOLZFÖRSTER, F. & STOLLHOFEN, H. 1999. Internal stratigraphic relationships in the Etendeka Group in the Huab Basin, NW Namibia: understanding the onset of flood volcanism. *Journal of Geodynamics*, **28**, 393–418.

JERRAM, D.A., MOUNTNEY, N., HOWELL, J., LONG, D. & STOLLHOFEN, H. 2000. Death of a Sand Sea: an active erg systematically buried by the Etendeka flood basalts of NW Namibia. *Journal of the Geological Society, London*, **157**, 513–516, https://doi.org/10.1144/jgs.157.3.513

JERRAM, D.A., DAVIS, G.R., MOCK, A., CHARRIER, A. & MARSH, B. 2010. Quantifying 3D crystal populations, packing and layering in shallow intrusions: a case study from the Basement Sill, Dry Valleys, Antarctica. *Geosphere*, **6**, 537–548, https://doi.org/10.1130/GES00538.1

JERRAM, D.A., SVENSEN, H.H., PLANKE, S., POLOZOV, A.G. & TORSVIK, T.H. 2016*a*. The onset of flood volcanism in the north-western part of the Siberian traps: explosive volcanism v. effusive lava flows. *Palaeogeography, Palaeoclimatology, Palaeoecology*, **441**, 38–50.

JERRAM, D.A., WIDDOWSON, M., WIGNALL, P.B., SUN, Y., LAI, X., BOND, D.P.G. & TORSVIK, T.H. 2016*b*. Submarine palaeoenvironments during Emeishan flood basalt volcanism, SW China: Implications for plume-lithosphere interaction during the Capitanian, Middle Permian ('end Guadalupian') extinction event. *Palaeogeography, Palaeoclimatology, Palaeoecology*. ISSN 0031-0182, **441**, 65–73. https://doi.org/10.1016/j.palaeo.2015.06.009

JONES, M.T., JERRAM, D.A., SVENSEN, H.H. & GROVE, C. 2016. The effects of large igneous provinces on the global carbon and sulphur cycles. *Palaeogeography, Palaeoclimatology, Palaeoecology*, **441**, 4–21.

JOURDAN, F., FÉRAUD, G. *ET AL.* 2004. The Karoo triple junction questioned: evidence from $^{40}Ar/^{39}Ar$ Jurassic and Proterozoic ages and geochemistry of the Okavango dike swarm (Botswana). *Earth and Planetary Science Letters*, **222**, 989–1006.

JOURDAN, F., FERAUD, G., BERTRAND, H., KAMPUNZU, A.B., TSHOSO, G., WATKEYS, M.K. & LE GALL, B. 2005. The Karoo large igneous province: brevity, origin, and relation with mass extinction questioned by new $^{40}Ar/^{39}Ar$ age data. *Geology*, **33**, 745–748.

JOURDAN, F., FÉRAUD, G., BERTRAND, H. & WATKEYS, M.K. 2007*a*. From flood basalts to the inception of oceanization: example from the $^{40}Ar/^{39}Ar$ high-resolution picture of the Karoo large igneous province. *Geochemistry, Geophysics, Geosystems*, **8**, 1–20, https://doi.org/10.1029/2006GC001392

JOURDAN, F., FÉRAUD, G., BERTRAND, H., WATKEYS, M.K. & RENNE, P.R. 2007*b*. Distinct brief major events in the Karoo large igneous province clarified by new $^{40}Ar/^{39}Ar$ ages on the Lesotho basalts. *Lithos*, **98**, 195–209.

JOURDAN, F., FÉRAUD, G., BERTRAND, H., WATKEYS, M.K. & RENNE, P.R. 2008. The $^{40}Ar/^{39}Ar$ ages of the sill complex of the Karoo large igneous province: implications for the Pliensbachian–Toarcian climate change. *Geochemistry, Geophysics, Geosystems*, **9**, 1–20, https://doi.org/10.1029/2008GC001994

JOURDAN, F., MARZOLI, A. *ET AL.* 2009. $^{40}Ar/^{39}Ar$ ages of CAMP in North America: implications for the Triassic–Jurassic boundary and the ^{40}K decay constant bias. *Lithos*, **110**, 167–180.

JOURDAN, F., HODGES, K. *ET AL.* 2014. High-precision dating of the Kalkarindji large igneous province, Australia, and synchrony with the Early–Middle Cambrian (Stage 4–5) extinction. *Geology*, **42**, 543–546.

KNIGHT, K.B., NOMADE, S., RENNE, P.R., MARZOLI, A., BERTRAND, H. & YOUBI, N. 2004. The Central Atlantic Magmatic Province at the Triassic–Jurassic boundary: paleomagnetic and $^{40}Ar/^{39}Ar$ evidence from Morocco for brief, episodic volcanism. *Earth and Planetary Science Letters*, **228**, 143–160.

KUIPER, K.F., DEINO, A., HILGEN, F.J., KRIJGSMAN, W., RENNE, P.R. & WIJBRANS, J.R. 2008. Synchronizing rock clocks of Earth history. *Science*, **320**, 500–504.

LANDING, E., BOWRING, S.A., DAVIDEK, K.L., WESTROP, S.R., GEYER, G. & HELDMAIER, W. 1998. Duration of the Early Cambrian: U–Pb ages of volcanic ashes from Avalon and Gondwana. *Canadian Journal of Earth Sciences*, **35**, 329–338, https://doi.org/10.1139/e97-107

LE GALL, B., TSHOSO, G. *ET AL.* 2002. $^{40}Ar/^{39}Ar$ geochronology and structural data from the giant Okavango and related mafic dike swarms, Karoo igneous province, Botswana. *Earth and Planetary Science Letters*, **202**, 595–606.

LUTTRELL, G.W. 1989. Stratigraphic nomenclature of the Newark supergroup of eastern North America. United States Geological Survey Bulletin 1572, 136 p.

MARSH, B.D. 2004. A magmatic mush column rosetta stone: the McMurdo Dry Valleys of Antarctica. *Eos, Transactions of the American Geophysical Union*, **85**, 497–508, https://doi.org/10.1029/2004EO470001

MARSH, J.S. & EALES, H.V. 1984. The chemistry and Petrogenesis of igneous rocks of the Karoo central area, southern Africa. *In*: ERLANK, A.J. (ed.) *Petrogenesis of the Volcanic Rocks of the Karoo Province*. Geological Society of South Africa, Special Publications, **13**, 27–67.

MARSH, J.S., HOOPER, P.R., REHACEK, J. & DUNCAN, R.A. 1997. Stratigraphy and age of the Karoo basalts of Lesotho and implications for correlations within the Karoo igneous province. *In*: MAHONEY, J.J. & COFFIN, M.F. (eds) *Large Igneous Provinces: Continental, Oceanic, and Planetary Flood Volcanism*. American Geophysical Union, Geophysical Monograph Series, **100**, 247–272.

MARSH, J.S., EWART, A., MILNER, S.C., DUNCAN, A.R. & MILLER, R.McG. 2001. The Etendeka Igneous Province: magma types and their stratigraphic distribution with implications for the evolution of the Paraná–Etendeka flood basalt province. *Bulletin of Volcanology*, **62**, 464–486.

MARSHALL, P.E., WIDDOWSON, M. & MURPHY, D.T. 2016. The Giant Lavas of Kalkarindji: rubbly pāhoehoe lava in an ancient continental flood basalt province. *Palaeogeography, Palaeoclimatology, Palaeoecology*, **441**, 22–37.

MARTINEZ, M., DECONINCK, J.F., PELLENARD, P., RIQUIER, L., COMPANY, M., REBOULET, S. & MOIROUD, M. 2015. Astrochronology of the Valanginian–Hauterivian stages (Early Cretaceous): chronological relationships between the Paraná–Etendeka large igneous province and the Weissert and the Faraoni events. *Global and Planetary Change*, **131**, 158–173.

MARZOLI, A., MELLUSO, L. *ET AL.* 1999*a*. Geochronology and petrology of Cretaceous basaltic magmatism in the Kwanza basin (western Angola), and relationships with the Parana–Etendeka continental flood basalt province. *Journal of Geodynamics*, **28**, 341–356.

MARZOLI, A., RENNE, P.R., PICCIRILLO, E.M., ERNESTO, M., BELLIENI, G. & DE MIN, A. 1999*b*. Extensive 200-million-year-old continental flood basalts of the Central Atlantic Magmatic Province. *Science*, **284**, 616–618.

MARZOLI, A., BERTRAND, H. *ET AL.* 2004. Synchrony of the Central Atlantic magmatic province and the Triassic–Jurassic boundary climatic and biotic crisis. *Geology*, **32**, 973–976.

MARZOLI, A., JOURDAN, F. *ET AL.* 2011. Timing and duration of the Central Atlantic magmatic province in the Newark and Culpeper basins, eastern USA. *Lithos*, **122**, 175–188.

MARSHALL, P.E., WIDDOWSON, M. & MURPHY, D.T. 2016. The Giant Lavas of Kalkarindji: rubbly pāhoehoe lava in an ancient continental flood basalt province. *Palaeogeography, Palaeoclimatology, Palaeoecology*, **441**, 22–37, https://doi.org/10.1016/j.palaeo.2015.05.006

MCCLINTOCK, M. & WHITE, J.D.L. 2006. Large phreatomagmatic vent complex at Coombs Hills, Antarctica: wet. explosive initiation of flood basalt volcanism in the Ferrar–Karoo LIP. *Bulletin of Volcanology*, **68**, 215–239.

MCCLINTOCK, M., WHITE, J.D.L., HOUGHTON, B.F. & SKILLING, I.P. 2008. Physical volcanology of a large crater-complex formed during the initial stages of Karoo flood basalt volcanism, Sterkspruit, Eastern Cape, South Africa. *Journal of Volcanology and Geothermal Research*, **172**, 93–111.

MCHONE, G. 1996. Broad terrane Jurassic flood basalts across northeastern North America. *Geology*, **24**, 319–322.

MCHONE, J.G. 2003. Volatile emissions from Central Atlantic Magmatic Province Basalts: mass assumptions and environmental consequences. *In*: HAMES, W., MCHONE, J.G., RENNE, P.C. & RUPPEL, C. (eds) *The Central Atlantic Magmatic Province: Insights from Fragments of Pangea*. American Geophysical Union, Geophysical Monograph Series, **136**, 241–254.

MEDLICOTT, H.B. & BLANFORD, W.T. 1879. *Manual of the Geology of India Pt. 1*. Geological Survey Office, Calcutta.

MERLE, R., MARZOLI, A. *ET AL.* 2011. $^{40}Ar/^{39}Ar$ ages and Sr–Nd–Pb–Os geochemistry of CAMP tholeiites from Western Maranhão basin (NE Brazil). *Lithos*, **122**, 137–151.

MERLE, R., MARZOLI, A. *ET AL.* 2014. Sr, Nd, Pb and Os isotope systematics of CAMP tholeiites from Eastern North America (ENA): evidence of a subduction-enriched mantle source. *Journal of Petrology*, **55**, 133–180.

MILANI, E.J. & ZALÁN, P.V. 1999. An outline of the geology and petroleum systems of the Paleozoic interior basins of South America. *Episodes*, **22**, 199–205.

MIZUSAKI, A.M.P., THOMAZ-FILHO, A., MILANI, E.J. & DE CÉSERO, P. 2002. Mesozoic and Cenozoic igneous activity and its tectonic control in northeastern Brazil. *Journal of South American Earth Sciences*, **15**, 183–198.

MOUNTNEY, N., HOWELL, J., FLINT, S. & JERRAM, D. 1998. Aeolian and alluvial deposition within the Mesozoic Etjo Sandstone Formation, northwest Namibia. *Journal of African Earth Sciences*, **27**, 175–192.

MUIRHEAD, J.D., AIROLDI, G., WHITE, J.D.L. & ROWLAND, J.V. 2014. Cracking the lid: sill-fed dikes are the likely feeders of flood basalt eruptions. *Earth and Planetary Science Letters*, **406**, 187–197.

NEUMANN, E.-R., SVENSEN, H., GALERNE, C.Y. & PLANKE, S. 2011. Multistage evolution of dolerites in the Karoo Large Igneous Province, Central South Africa. *Journal of Petrology*, **52**, 959–984.

NOMADE, S., THÉVENIAUT, H., CHEN, Y., POUCLET, A. & RIGOLLET, C. 2000. Paleomagnetic study of French Guyana Early Jurassic dolerites: hypothesis of a multistage magmatic event. *Earth and Planetary Science Letters*, **184**, 155–168.

NOMADE, S., KNIGHT, K.B. *ET AL.* 2007. Chronology of the Central Atlantic Magmatic Province: implications for the Central Atlantic rifting processes and the Triassic–Jurassic biotic crisis. *Palaeogeography, Palaeoclimatology, Palaeoecology*, **244**, 326–344.

PÁLFY, J., SMITH, P.L. & MORTENSEN, J.K. 2000. A U–Pb and $^{40}Ar/^{39}Ar$ time scale for the Jurassic. *Canadian Journal of Earth Sciences*, **37**, 923–944.

PARISIO, L., JOURDAN, F. *ET AL.* 2016. $^{40}Ar/^{39}Ar$ ages of alkaline and tholeiitic rocks from the northern Deccan Traps: implications for magmatic processes and the K–Pg boundary. *Journal of the Geological Society, London*, **173**, 679–688, https://doi.org/10.1144/jgs2015-133

PEATE, D.W. 1997. The Parana-Etendeka Province. *In*: MAHONEY, J.J. & COFFIN, M.F. (eds) *Large Igneous Provinces*. American Geophysical Union, Washington, DC, 217–245.

PEATE, D.W. & HAWKESWORTH, C.J. 1996. Lithospheric to asthenospheric transition in Low-Ti flood basalts from southern Paranà & Brazil. *Chemical Geology*, **127**, 1–24.

PETRY, K., JERRAM, D.A., DEL PILAR, M.D. & ZERFASS, H. 2007. Volcanic–sedimentary features in the Serra Geral Fm., Paraná Basin, southern Brazil: examples of dynamic lava–sediment interactions in an arid setting. *Journal of Volcanology and Geothermal Research*, **159**, 313–325.

POLTEAU, S., FERRÉ, E., PLANKE, S., NEUMANN, E.-R. & CHEVALLIER, L. 2008. How are saucer-shaped sills emplaced? Constraints from the Golden Valley Sill, South Africa. *Journal of Geophysical Research*, **113**, B12104, https://doi.org/10.1029/2008JB005620

PORTO, A. & PEREIRA, E. 2014. Seismic interpretation of igneous intrusions and their implications for an unconventional petroleum system in southeastern Parnaiba Basin, northeastern Brazil. Abstract V51B presented at *American Geophysical Union Fall Meeting 2014*, 15–19 December 2014, San Francisco, CA, USA.

PUFFER, J.H., BLOCK, K.A. & STEINER, J.C. 2009. Transmission of flood basalts through a shallow crustal sill and the correlation of sill layers with extrusive flows: the Palisades intrusive system and the basalts of the Newark Basin, New Jersey, U. S. A. *Journal of Geology*, **117**, 139–155.

RENNE, P.R., GLEN, J.M., MILNER, S.C. & DUNCAN, A.R. 1996. Age of Etendeka flood volcanism and associated intrusions in southwestern Africa. *Geology*, **24**, 659–662.

RENNE, P.R., MUNDIL, R., BALCO, G., MIN, K. & LUDWIG, K. R. 2010. Joint determination of ^{40}K decay constants and $^{40}Ar^*/^{40}K$ for the Fish Canyon sanidine standard, and improved accuracy for $^{40}Ar/^{39}Ar$ geochronology. *Geochimica et Cosmochimica Acta*, **74**, 5349–5367.

ROBOCK, A. 2005. Cooling following large volcanic eruptions corrected for the effect of diffuse radiation on tree rings. *Geophysical Research Letters*, **32**, L06702.

ROYER, D.L. 2006. CO_2-forced climate thresholds during the Phanerozoic. *Geochimica et Cosmochimica Acta*, **70**, 5665–5675.

SCHOENE, B., CROWLEY, J.L., CONDON, D.J., SCHMITZ, M.D. & BOWRING, S.A. 2006. Reassessing the uranium decay constants for geochronology using ID-TIMS U–Pb data. *Geochimica et Cosmochimica Acta*, **70**, 426–445.

SCHOENE, B., GUEX, J., BARTOLINI, A., SCHALTEGGER, U. & BLACKBURN, T.J. 2010. Correlating the end- Triassic mass extinction and flood basalt volcanism at the 100 ka level. *Geology*, **38**, 387, https://doi.org/10.1130/G30683.1

SEBAI, A., FERAUD, G., BERTRAND, H. & HANES, J. 1991. ^{40}Ar–^{39}Ar dating and geochemistry of tholeiitic magamatism related to the early opening of the Central Atlantic rift. *Earth and Planetary Science Letters*, **194**, 455–472.

SELF, S., WIDDOWSON, M., THORDARSON, T. & JAY, A.E. 2006. Volatile fluxes during flood basalt eruptions and potential effects on the global environment: a Deccan perspective. *Earth and Planetary Science Letters*, **248**, 518–532.

SELL, B., OVTCHAROVA, M. *ET AL.* 2014. Evaluating the temporal link between the Karoo LIP and climatic–biologic events of the Toarcian Stage with high-precision U–Pb geochronology. *Earth and Planetary Science Letters*, **408**, 48–56.

SOBOLEV, S.V., SOBOLEV, A.V. *ET AL.* 2011. Linking mantle plumes, large igneous provinces and environmental catastrophes. *Nature*, **477**, 312–316.

STOREY, B.C., VAUGHAN, A.P.M. & RILEY, T.R. 2013. The links between large igneous provinces, continental break-up and environmental change: evidence reviewed from Antarctica. *Earth and Environmental Science, Transactions of the Royal Society of Edinburgh*, **104**, 17–30.

SUAN, G., PITTET, B., BOUR, I., MATTOILI, E., DUARTE, L.V. & MAILLIOT, S. 2008. Duration of the Early Toarcian carbon isotope excursion deduced from spectral analysis: consequence for its possible causes. *Earth and Planetary Science Letters*, **267**, 666–679, https://doi.org/10.1016/j.epsl.2007.12.017

SVENSEN, H., PLANKE, S. & MALTHE-SØRENSSEN, A. 2004. Release of methane from a volcanic basin as a mechanism for initial Eocene global warming. *Nature*, **429**, 3–6.

SVENSEN, H., JAMTVEIT, B., PLANKE, S. & CHEVALLIER, L. 2006. Structure and evolution of hydrothermal vent complexes in the Karoo Basin, South Africa. *Journal of the Geological Society, London*, **163**, 671–682, https://doi.org/10.1144/1144-764905-037

SVENSEN, H., PLANKE, S., CHEVALLIER, L., MALTHE-SØRENSSEN, A., CORFU, B. & JAMTVEIT, B. 2007. Hydrothermal venting of greenhouse gases triggering Early Jurassic global warming. *Earth and Planetary Science Letters*, **256**, 554–566.

SVENSEN, H., PLANKE, S., POLOZOV, A.G., SCHMIDBAUER, N., CORFU, F., PODLADCHIKOV, Y.Y. & JAMTVEIT, B. 2009. Siberian gas venting and the end-Permian environmental crisis. *Earth and Planetary Science Letters*, **277**, 490–500.

SVENSEN, H., CORFU, F., POLTEAU, S., HAMMER, Ø. & PLANKE, S. 2012. Rapid magma emplacement in the Karoo Large Igneous Province. *Earth and Planetary Science Letters*, **325–326**, 1–9. https://doi.org/10.1016/j.epsl.2012.01.015

Svensen, H.H., Hammer, Ø. & Corfu, F. 2015*a*. Astronomically forced cyclicity in the Upper Ordovician and U–Pb ages of interlayered tephra, Oslo Region, Norway. *Palaeogeography, Palaeoclimatology, Palaeoecology*, **418**, 150–159.

Svensen, H.H., Planke, S. *et al.* 2015*b*. Sub-volcanic intrusions and the link to global climatic and environmental changes. *In*: Breitkreuz, C. & Rocchi, S. (eds) *Physical Geology of Shallow Magmatic Systems*. ISBN: 978-3-319-14083-4. Springer International Publishing.

Svensen, H., Polteau, S., Cawthorn, G. & Planke, S. 2015*c*. Sub-volcanic intrusions in the Karoo Basin, South Africa. *In*: Breitkreuz, C. & Rocchi, S. (eds) *Physical Geology of Shallow Magmatic Systems*. ISBN: 978-3-319-14083-4. Springer International Publishing.

Tankard, A., Welsink, H., Aukes, P., Newton, R. & Stettler, E. 2009. Tectonic evolution of the Cape and Karoo basins of South Africa. *Marine and Petroleum Geology*, **26**, 1379–1412.

Thiede, D.S. & Vasconcelos, P.M. 2010. Parana flood basalts: rapid extrusion hypothesis confirmed by new $^{40}Ar/^{39}Ar$ results. *Geology*, **38**, 747–750.

Torsvik, T.H. & Cocks, L.R.M. 2013. GR focus review: Gondwana from top to base in space and time. *Gondwana Research*, **24**, 999–1030.

Torsvik, T.H. & Smethurst, M.A. 1999. Plate tectonic modeling: virtual reality with GMAP. *Computer & Geosciences*, **25**, 395–402.

Torsvik, T.H., Van der Voo, R. *et al.* 2012. Phanerozoic polar wander, paleogeography and dynamics. *Earth-Science Reviews*, **114**, 325–368.

Torsvik, T.H., Van der Voo, R. *et al.* 2014. Deep mantle structure as a reference frame for movements in and on the Earth. *Proceedings of the National Academy of Sciences of the United States of America*, **111**, 8735–8740.

Torsvik, T.H., Steinberger, B., Ashwal, L.D., Doubrovine, P.V. & Trønnes, R.C. 2016. Earth evolution and dynamics – a tribute to Kevin Burke. *Canadian Journal of Earth Sciences Special Issue*, **53**, 1073–1087, https://doi.org/10.1139/cjes-2015-0228

Vasiliev, Y.R., Zolotukhin, V.V., Feoktistov, G.D. & Prusskaya, S.N. 2000. Evaluation of the volume and genesis of Permo-Triassic Trap magmatism on the Siberian Platform. *Russian Geology and Geophysics*, **41**, 1696–1705.

Verati, C., Bertrand, H. & Féraud, G. 2005. The farthest record of the Central Atlantic Magmatic Province into West Africa craton: precise $^{40}Ar/^{39}Ar$ dating and geochemistry of Taoudenni basin intrusives (northern Mali). *Earth and Planetary Science Letters*, **235**, 391–407.

Visscher, H., Looy, C.V., Collinson, M.E., Brinkhuis, H., Cittert, J.H.A.V.K.V., Kurschner, W.M. & Sephton, M.A. 2004. Environmental mutagenesis during the end-Permian ecological crisis. *Proceedings of the National Academy of Sciences of the United States of America*, **101**, 12 952–12 956.

Waichel, B.L., Scherer, C.M.S. & Frank, H.T. 2008. Basaltic lavas covering active Aeolian dunes in the Paraná Basin in Southern Brazil: features and emplacement aspects. *Journal of Volcanology and Geothermal Research*, **169**, 59–72.

Waichel, B.L., de Lima, E.F., Viana, A.R., Scherer, C.M., Bueno, G.V. & Dutra, G. 2012. Stratigraphy and volcanic facies architecture of the Torres Syncline, Southern Brazil, and its role in understanding the Paraná–Etendeka Continental Flood Basalt Province. *Journal of Volcanology and Geothermal Research*, **215–216**, 74–82.

Wanderley Filho, J.R., Travassos, W.A.S. & Alves, D.B. 2006. O diabásio nas bacias paleozóicas amazônicas-herói ou vilão. [The diabase in the Amazonian Paleozoic basins: hero or villain?]. *Boletim de Geociências da Petrobrás*, **14**, 177–184.

White, J.D.L., Bryan, S.E., Ross, P.-S., Self, S. & Thordarson, T. 2009. Physical volcanology of continental large igneous provinces: update and review. *In*: Thordarson, T., Self, S., Larsen, G., Rowland, S.K. & Höskuldsson, A. (eds) *Studies in Volcanology: The Legacy of George Walker*. IAVCEI, Special Publications, **2**, 291–321.

Woodruff, L.G., Froelich, A.J., Belkin, H.E. & Gottfried, D. 1995. Evolution of tholeiitic diabase sheet systems in the eastern United States: examples from the Culpeper Basin, Virginia–Maryland, and the Gettysburg Basin, Pennsylvania. *Journal of Volcanology and Geothermal Research*, **64**, 143–169.